Multibosons at ATLAS and CMS

Saptaparna Bhattacharya

on behalf of the ATLAS and CMS collaborations

Humboldt Fellow, Wayne State Pathway-to-faculty Fellow

La Thuile, Moriond 2024

Vector Boson Scattering (VBS)

- Study of vector boson scattering processes → essential to probe nature of electroweak symmetry breaking
- Differential measurements performed and constraints on various effective field theory operators evaluated
- Several kinematic observables sensitive to the effect of new physics

- Pure electro-weak interactions of order α_{EW}^4

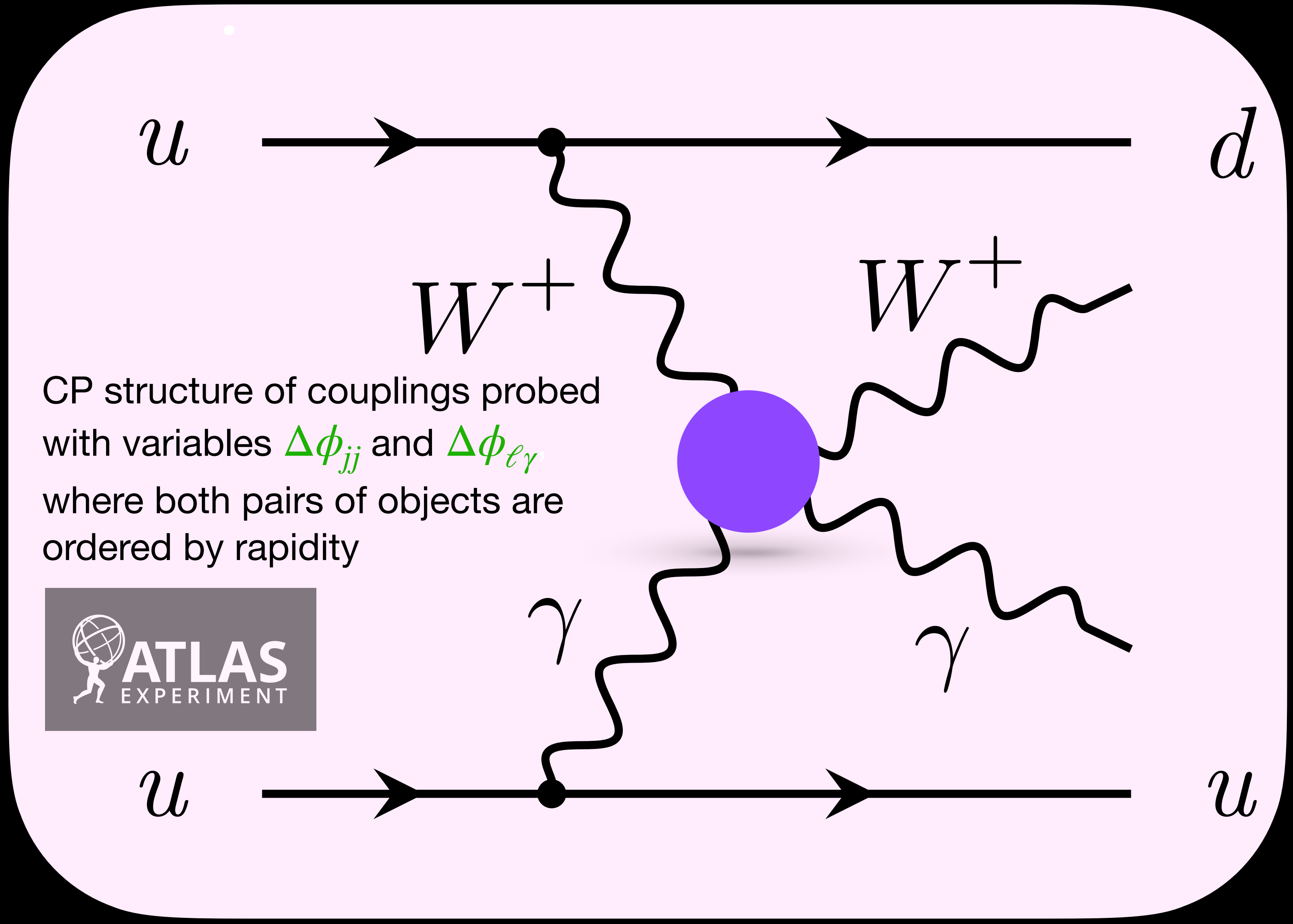

- Pure electro-weak interactions of order α_{EW}^6

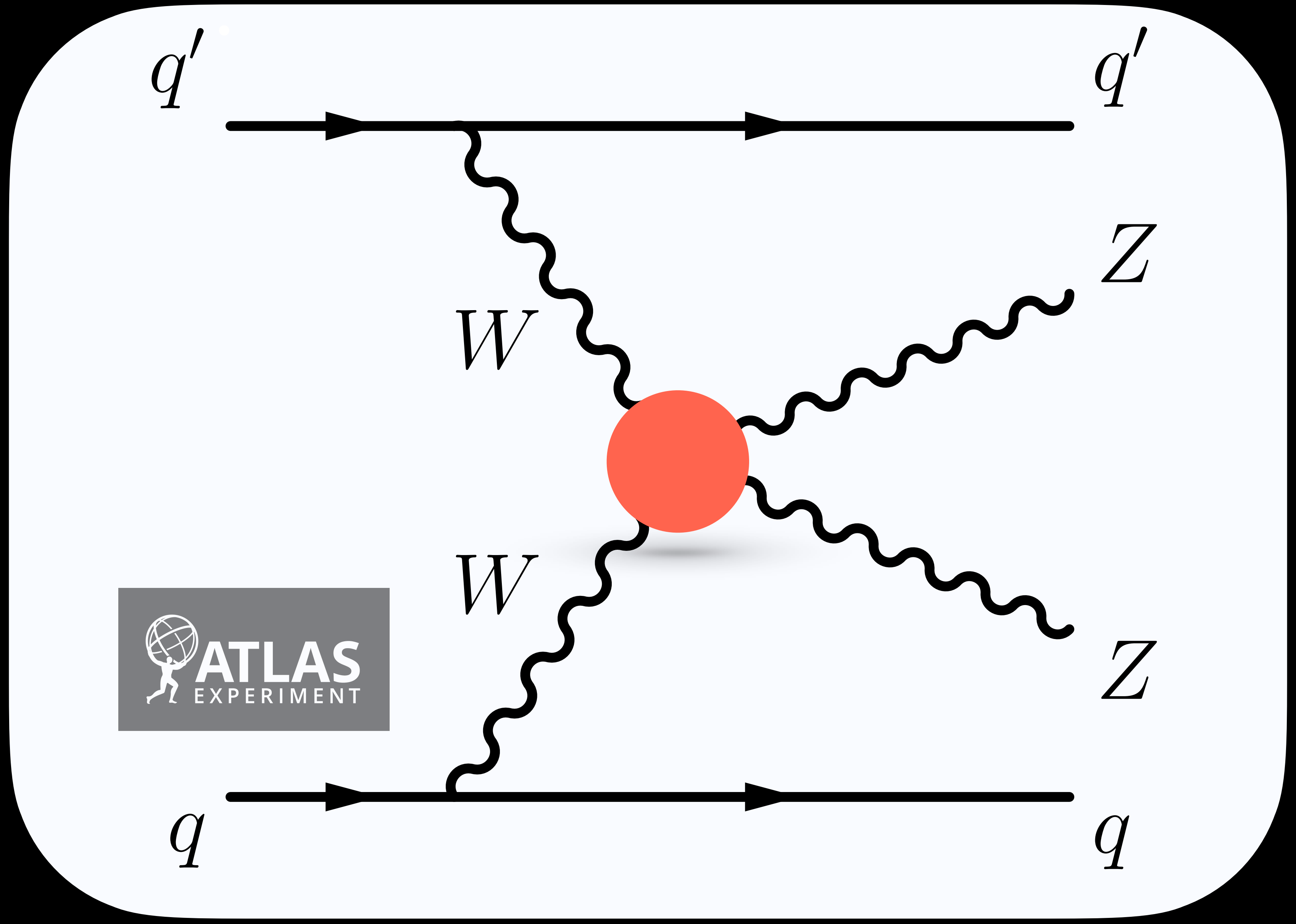

- Pure electro-weak interactions of order α_{EW}^6

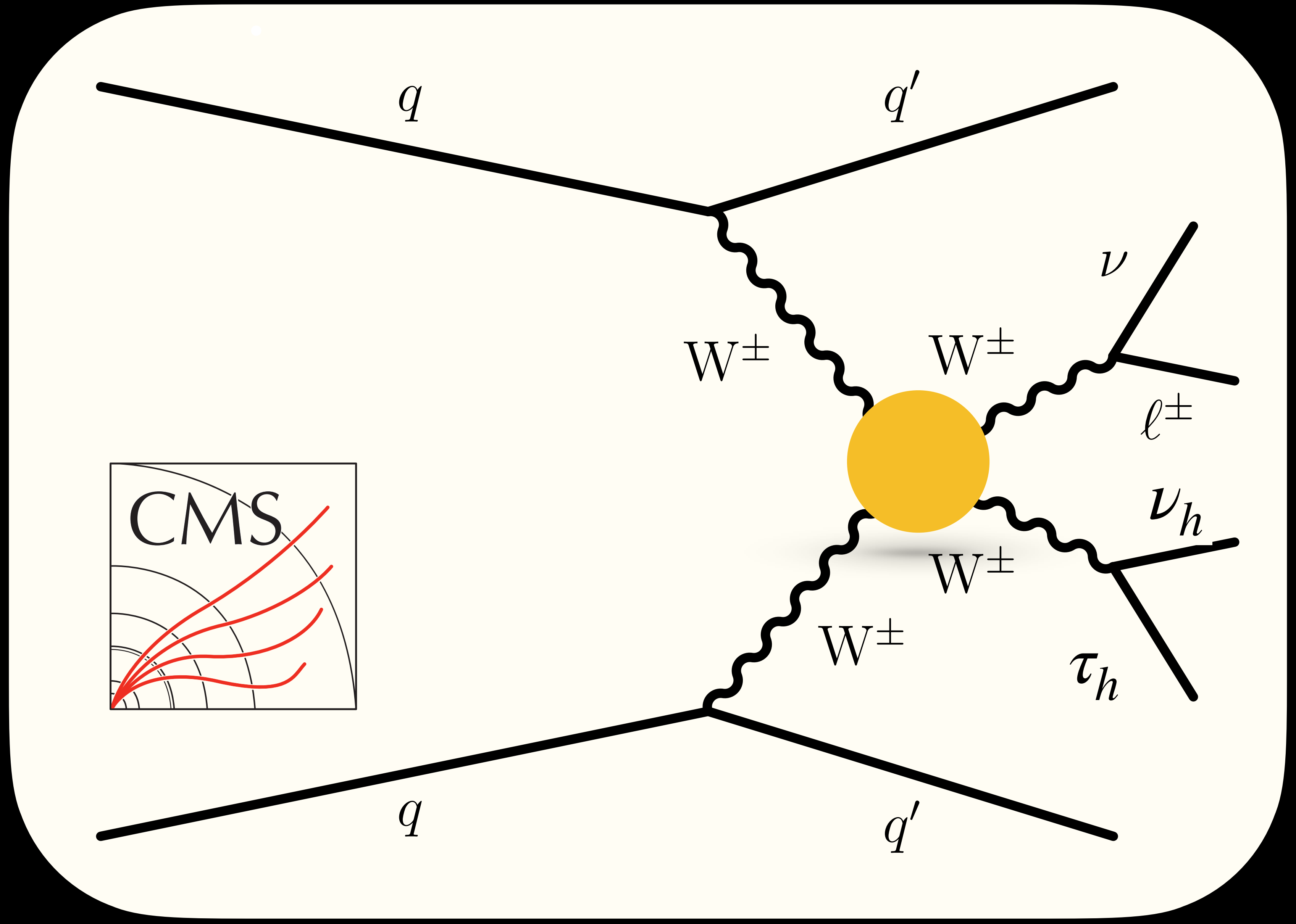

VBS $W\gamma$ at 13 TeV

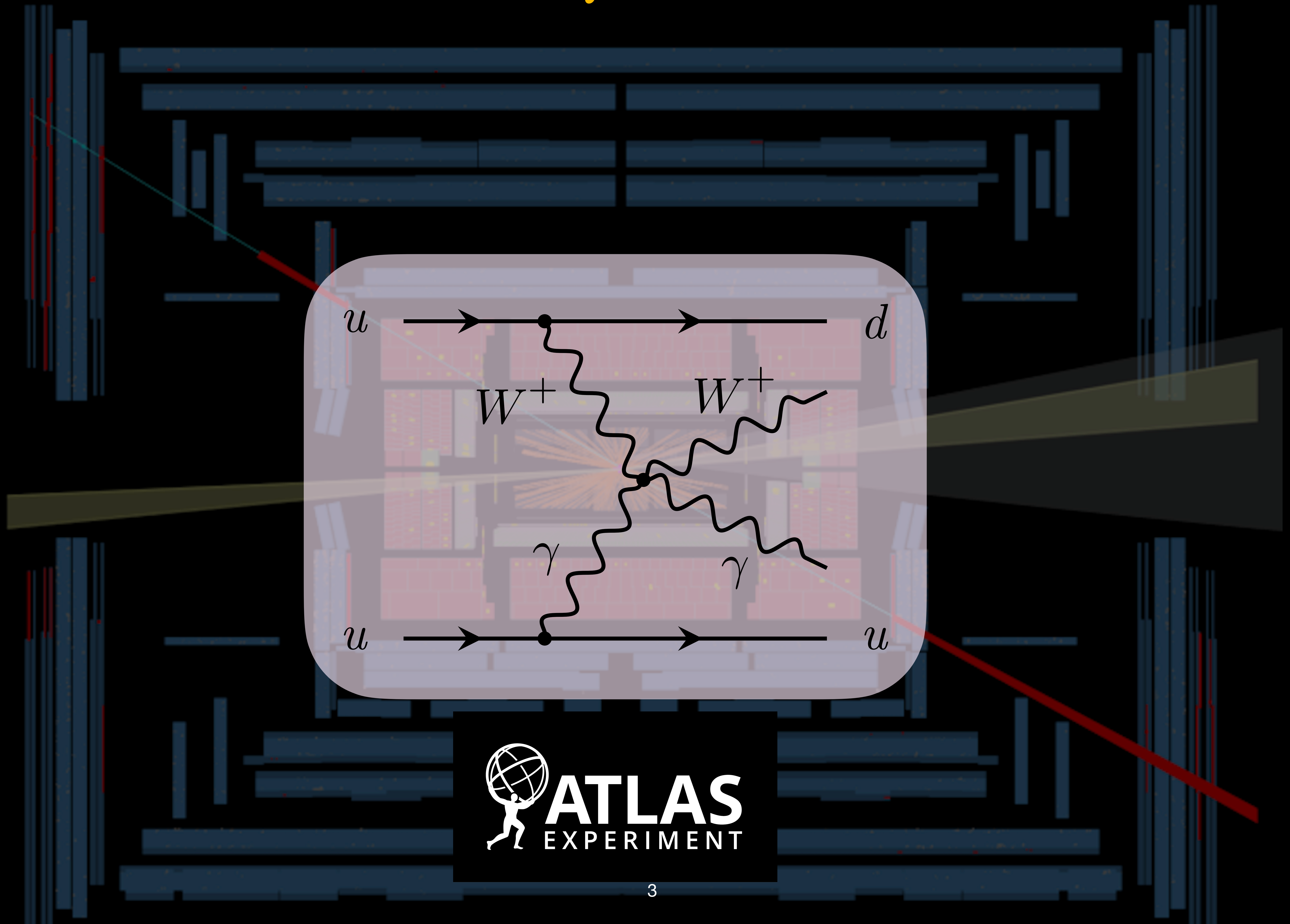

ATLAS EXPERIMENT

https://arxiv.org/abs/2403.02809

VBS $W\gamma$ at 13 TeV

- Neural Network trained with 13 angular and kinematic variables used to enhance sensitivity to EW $W\gamma jj$ (inclusive measurement)
- Signal region (SR) and control region (CR) defined by counting $N_{\text{jets}}^{\text{gap}}$ (rapidity interval between the two leading jets)
  - SR: $m_{jj} > 1$ TeV, $\xi_{\ell\gamma} = \left|(y_{\ell\gamma} - \frac{(y_{j_1} + y_{j_2})}{2})/(y_{j_1} - y_{j_2})\right| < 0.35$

The ABCD method is only used in the differential measurement

	$\text{SR}^{\text{fid}}\ (N_{\text{jets}}^{\text{gap}} = 0)$	$\text{CR}^{\text{fid}}\ (N_{\text{jets}}^{\text{gap}} > 0)$
EW $W\gamma jj$	520 ± 141	120 ± 49
Strong $W\gamma jj$	1550 ± 830	1970 ± 950
Non-prompt	692 ± 57	698 ± 58
Top quark processes	109 ± 18	183 ± 37
EW + strong $Z\gamma jj$	128 ± 34	163 ± 77
Total	3000 ± 830	3140 ± 960
Data	3341	3143

Highest ranked variables

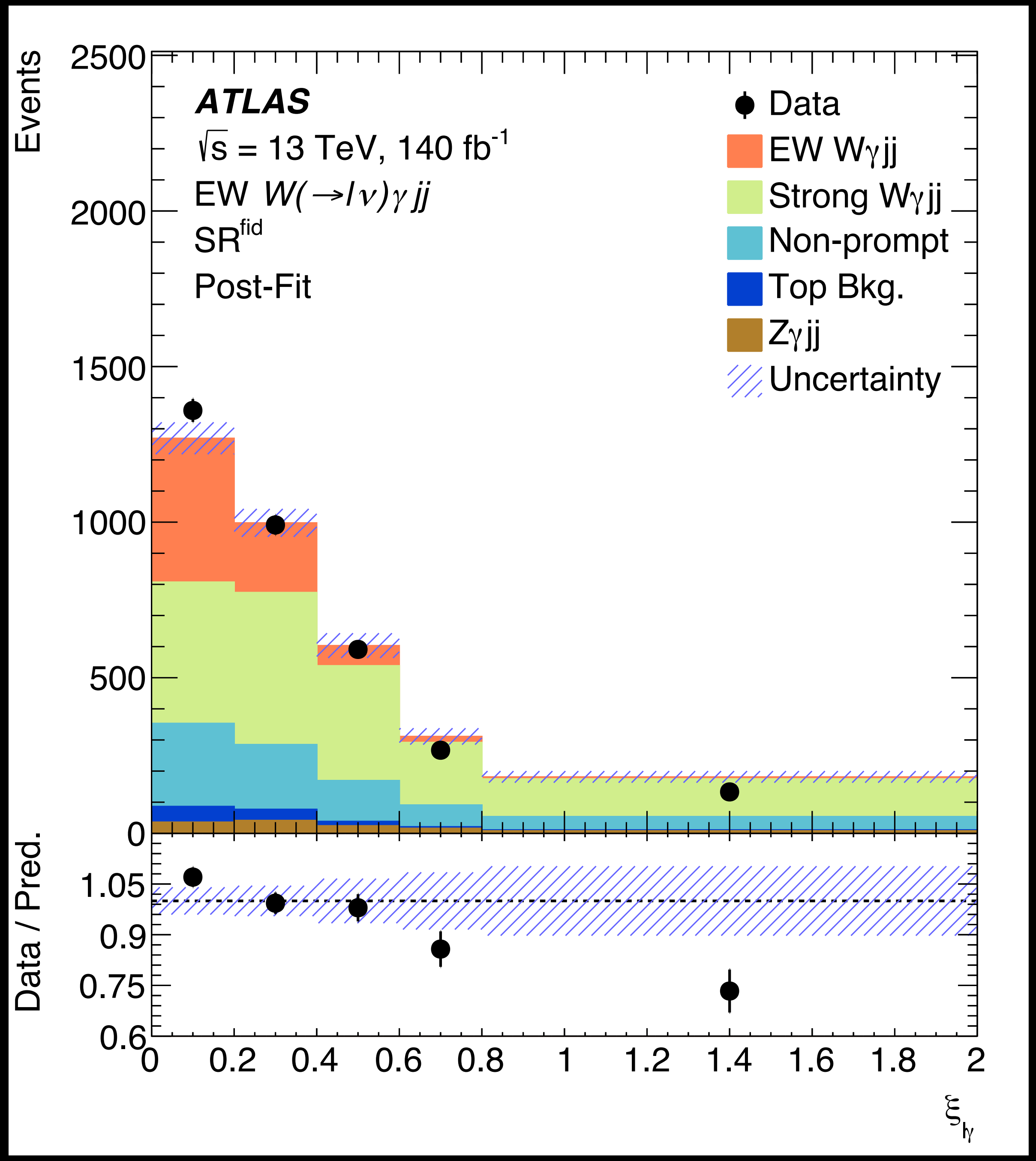

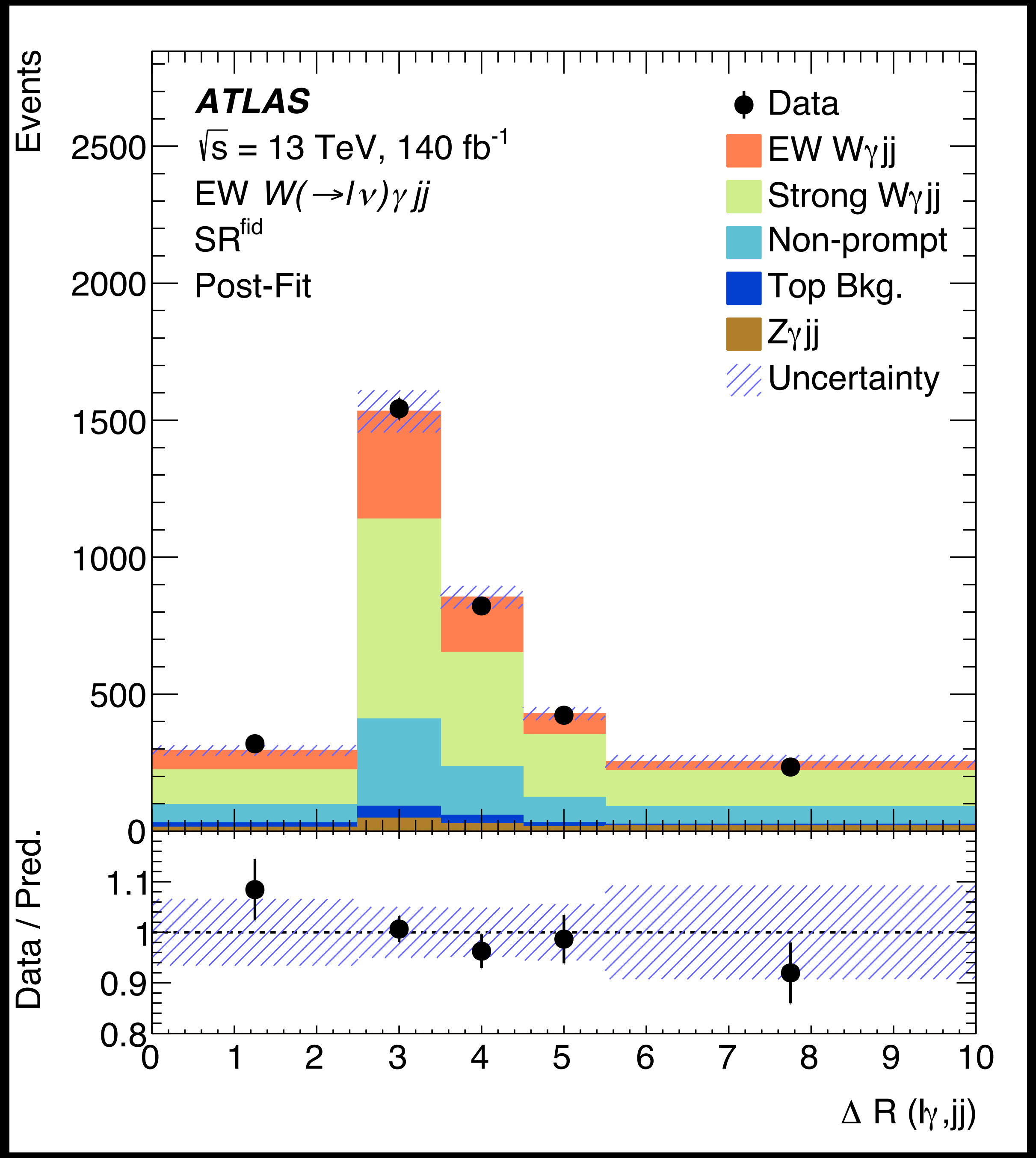

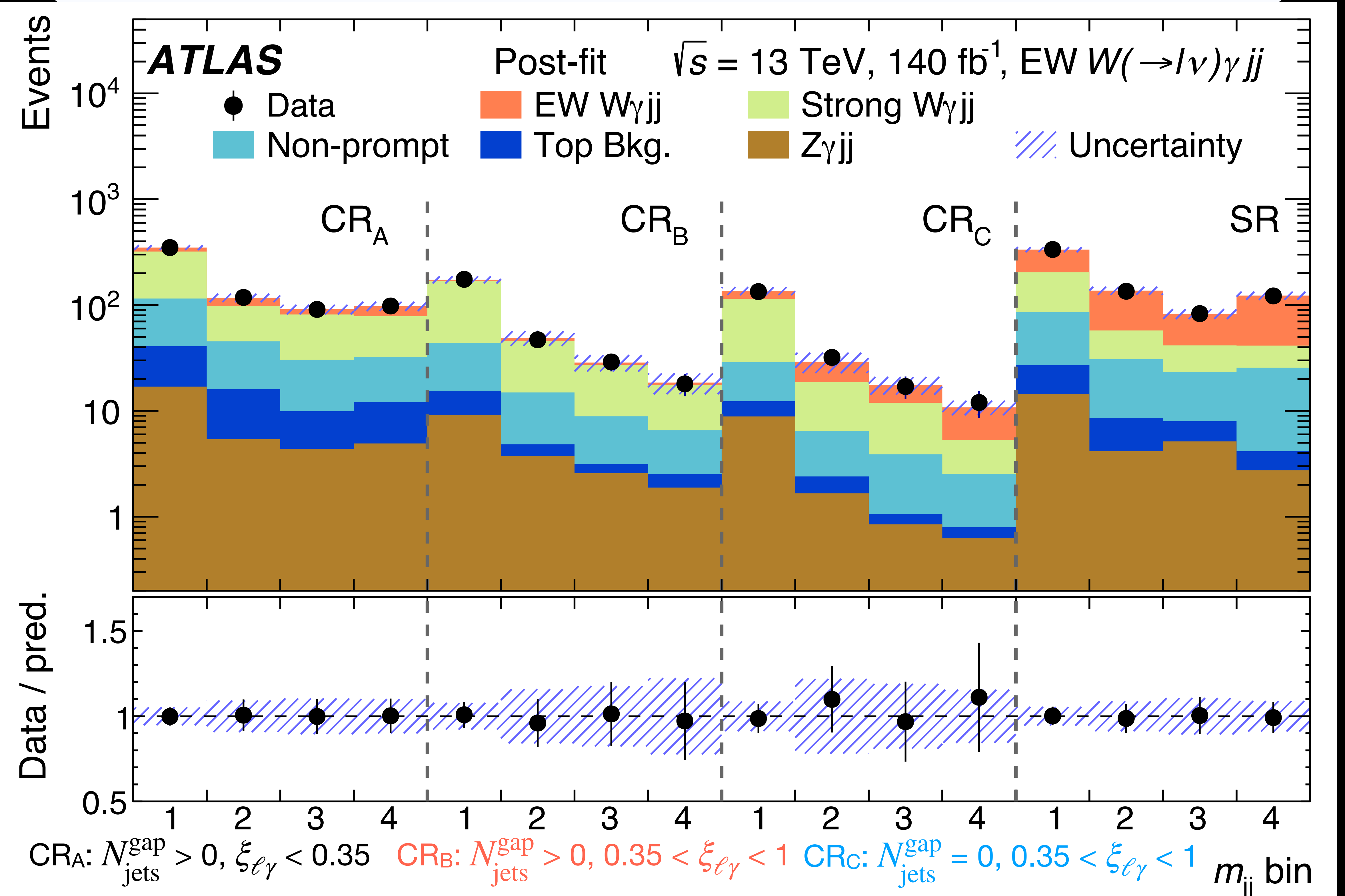

https://arxiv.org/abs/2403.02809

VBS $W\gamma$ at 13 TeV

- Particle level fiducial and differential cross sections obtained after de-convolving EW $W\gamma jj$ yield from detector effects
- Sherpa (2.2.12) and Madgraph5+Pythia8 used for comparison

https://arxiv.org/abs/2403.02809

VBS $W\gamma$ at 13 TeV

$$\mathscr{L}_{EFT} = \mathscr{L}_{SM} + \sum_i \frac{f_i^8}{\Lambda^4}\mathcal{O}^8$$

Differential cross section:

$$|\mathscr{M}|^2 = |\mathscr{M}_{SM}|^2 +$$

Pure SM

$$2Re(\mathscr{M}^*_{SM}\mathscr{M}_{D-8}) + |\mathscr{M}_{D-8}|^2$$

Interference between SM and BSM

Pure BSM

Pure D-8 terms affects differential cross section measurements significantly more than the interference term

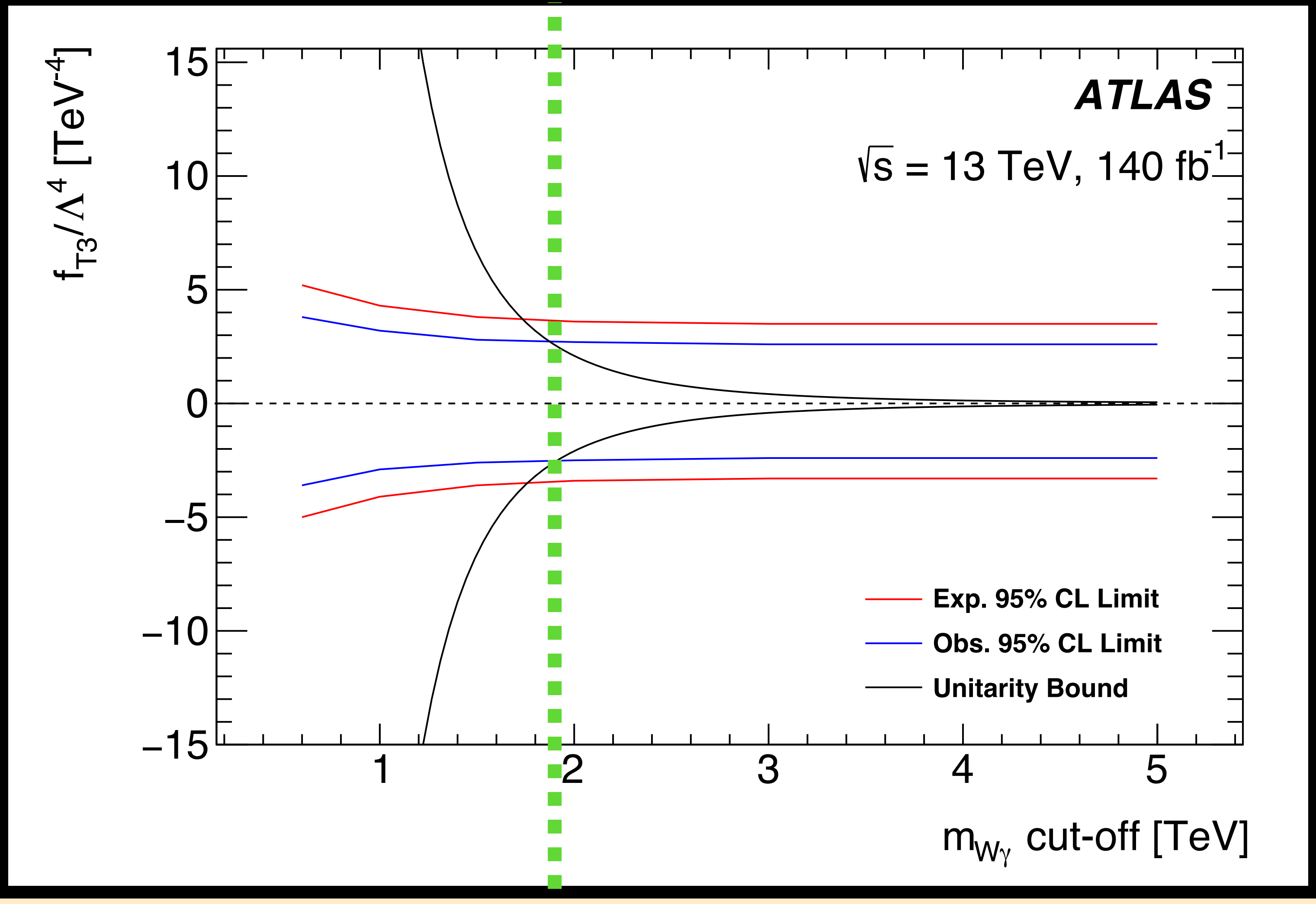

Cofficients [TeV^{-4}]	Observable	$M_{W\gamma}$ cut-off [TeV]	Expected [TeV^{-4}]	Observed [TeV^{-4}]
f_{T0}/Λ^4	p_T^{jj}	1.4	[-2.5, 2.6]	[-1.9, 1.9]
f_{T1}/Λ^4	p_T^{jj}	1.9	[-1.6, 1.6]	[-1.1, 1.2]
f_{T2}/Λ^4	p_T^{jj}	1.6	[-4.9, 5.3]	[-3.6, 4.0]
f_{T3}/Λ^4	p_T^{jj}	1.9	[-3.4, 3.6]	[-2.5, 2.7]
f_{T4}/Λ^4	p_T^{jj}	2.2	[-3.1, 3.1]	[-2.2, 2.3]
f_{T5}/Λ^4	p_T^{jj}	1.8	[-1.8, 1.8]	[-1.3, 1.3]
f_{T6}/Λ^4	p_T^{jj}	2.1	[-1.5, 1.5]	[-1.1, 1.1]
f_{T7}/Λ^4	p_T^{jj}	2.1	[-4.0, 4.1]	[-2.9, 3.0]
f_{M0}/Λ^4	p_T^{l}	1.1	[-45, 44]	[-32, 31]
f_{M1}/Λ^4	p_T^{l}	1.4	[-60, 62]	[-43, 44]
f_{M2}/Λ^4	p_T^{l}	1.4	[-15, 15]	[-11, 11]
f_{M3}/Λ^4	p_T^{l}	1.8	[-22, 22]	[-16, 16]
f_{M4}/Λ^4	p_T^{l}	1.5	[-28, 27]	[-20, 20]
f_{M5}/Λ^4	p_T^{l}	1.9	[-21, 23]	[-14, 17]
f_{M7}/Λ^4	p_T^{l}	1.5	[-100, 99]	[-73, 71]

VBS WZ at 13 TeV

https://arxiv.org/abs/2403.15296

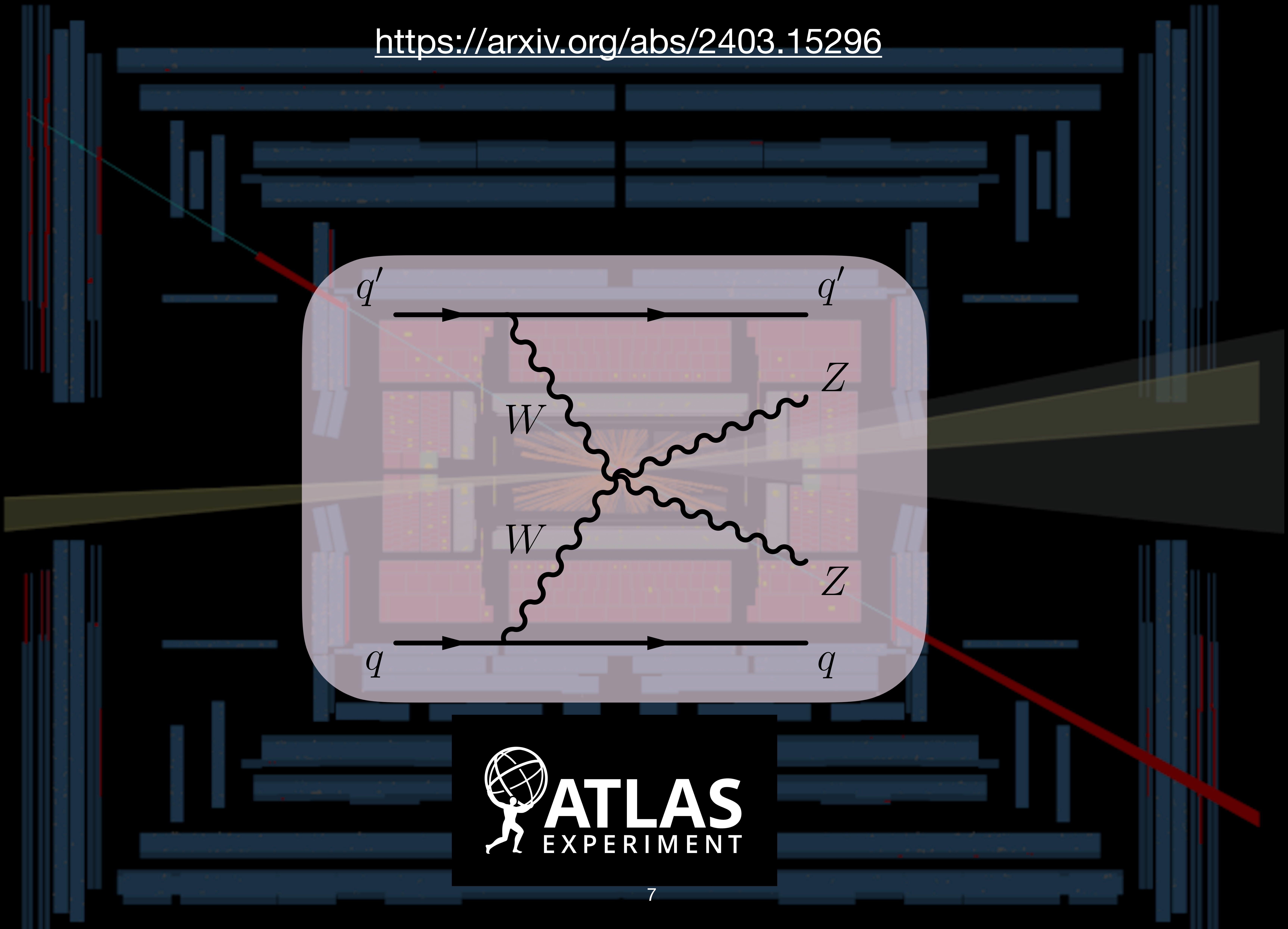

VBS WZ at 13 TeV

https://arxiv.org/abs/2403.15296

- Simultaneous extraction of EW $WZjj$ and QCD $WZjj$
- Sensitivity enhanced to EW $WZjj$ by using a BDT discriminant constructed with 15 variables as inputs (jet, vector boson and lepton kinematics)
    - Signal regions defined by $N_{\mathrm{jets}} = 2$ and $N_{\mathrm{jets}} \geq 3$ and in three bins of M_{jj} ($500 \leq M_{jj} < 1300$, $1300 \leq M_{jj} < 2000$, $M_{jj} \geq 2000$)
    - Adversarial neural network used to separate EW $WZjj$ and QCD $WZjj$ without biasing M_{jj}

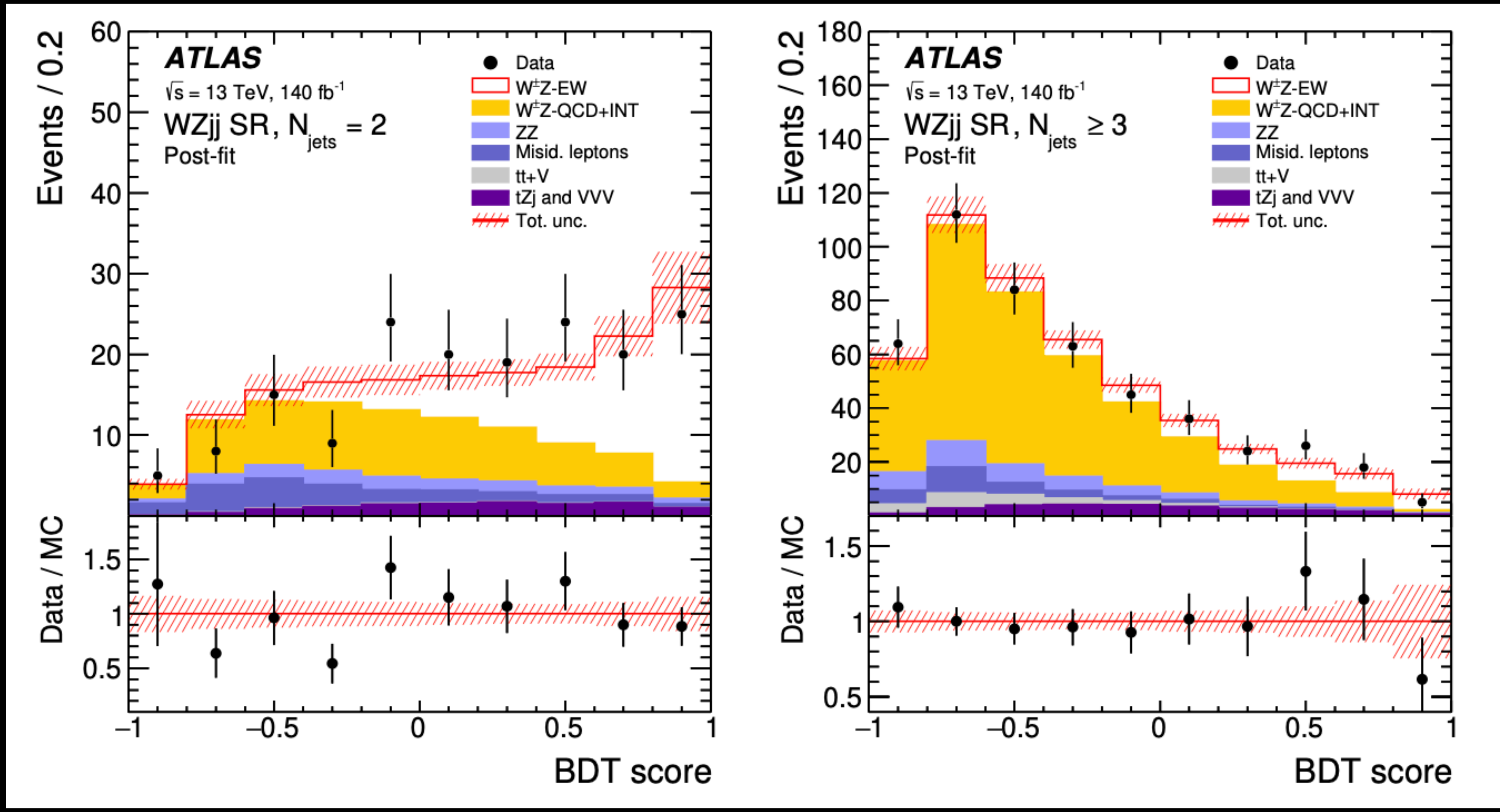

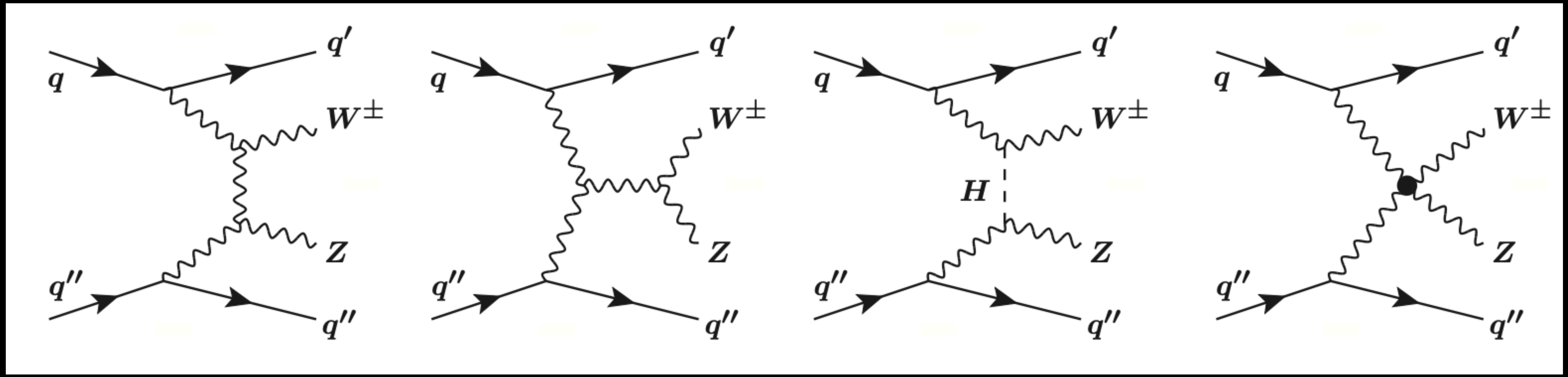

LO diagrams for EW $WZjj$

https://arxiv.org/abs/2403.15296

VBS WZ at 13 TeV

- Measured $\sigma_{WZjj-EW} = 0.368 \pm 0.037 \text{ (stat.)} \pm 0.059 \text{ (syst.)} \pm 0.003 \text{ (lumi.) fb}$
- Measured $\sigma_{WZjj-QCD} = 1.093 \pm 0.066 \text{ (stat.)} \pm 0.131 \text{ (syst.)} \pm 0.009 \text{ (lumi.) fb}$

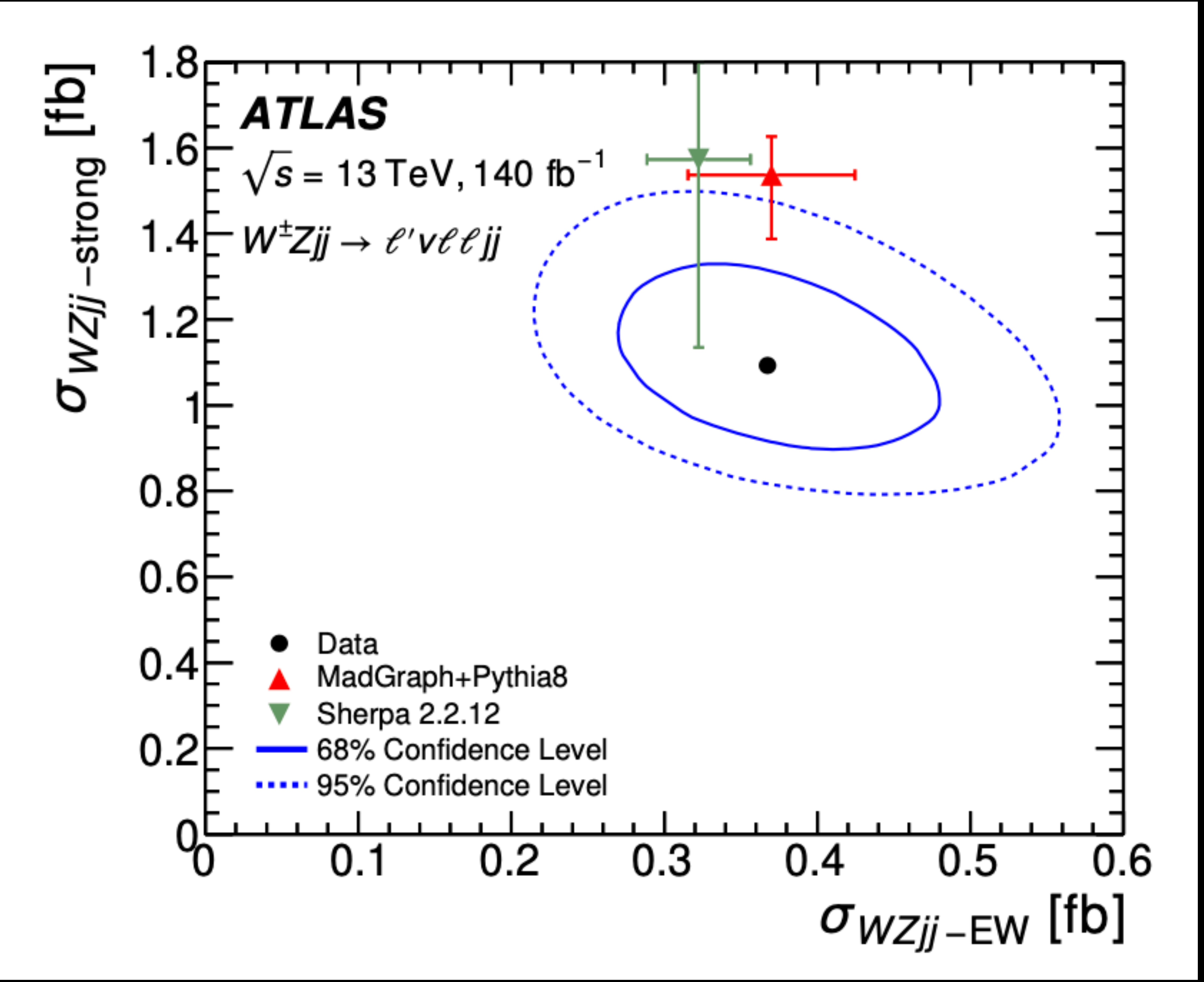

Integrated cross sections

Source	$\frac{\Delta\sigma_{WZjj\text{–EW}}}{\sigma_{WZjj\text{–EW}}}$ [%]	$\frac{\Delta\sigma_{WZjj\text{–strong}}}{\sigma_{WZjj\text{–strong}}}$ [%]
$WZjj$–EW theory modelling	7	1.8
$WZjj$–QCD theory modelling	2.8	8
$WZjj$–EW and $WZjj$–QCD interference	0.35	0.6
PDFs	1.0	0.06
Jets	2.3	5
Pile-up	1.1	0.6
Electrons	0.8	0.8
Muons	0.9	0.9
b-tagging	0.10	0.11
MC statistics	1.9	1.2
Misid. lepton background	2.3	2.3
Other backgrounds	0.9	0.23
Luminosity	0.7	0.9
All systematics	16	12
Statistics	10	6
Total	19	13

Correlations in $WZjj-EW$ and $WZjj-QCD$

https://arxiv.org/abs/2403.15296

VBS WZ at 13 TeV

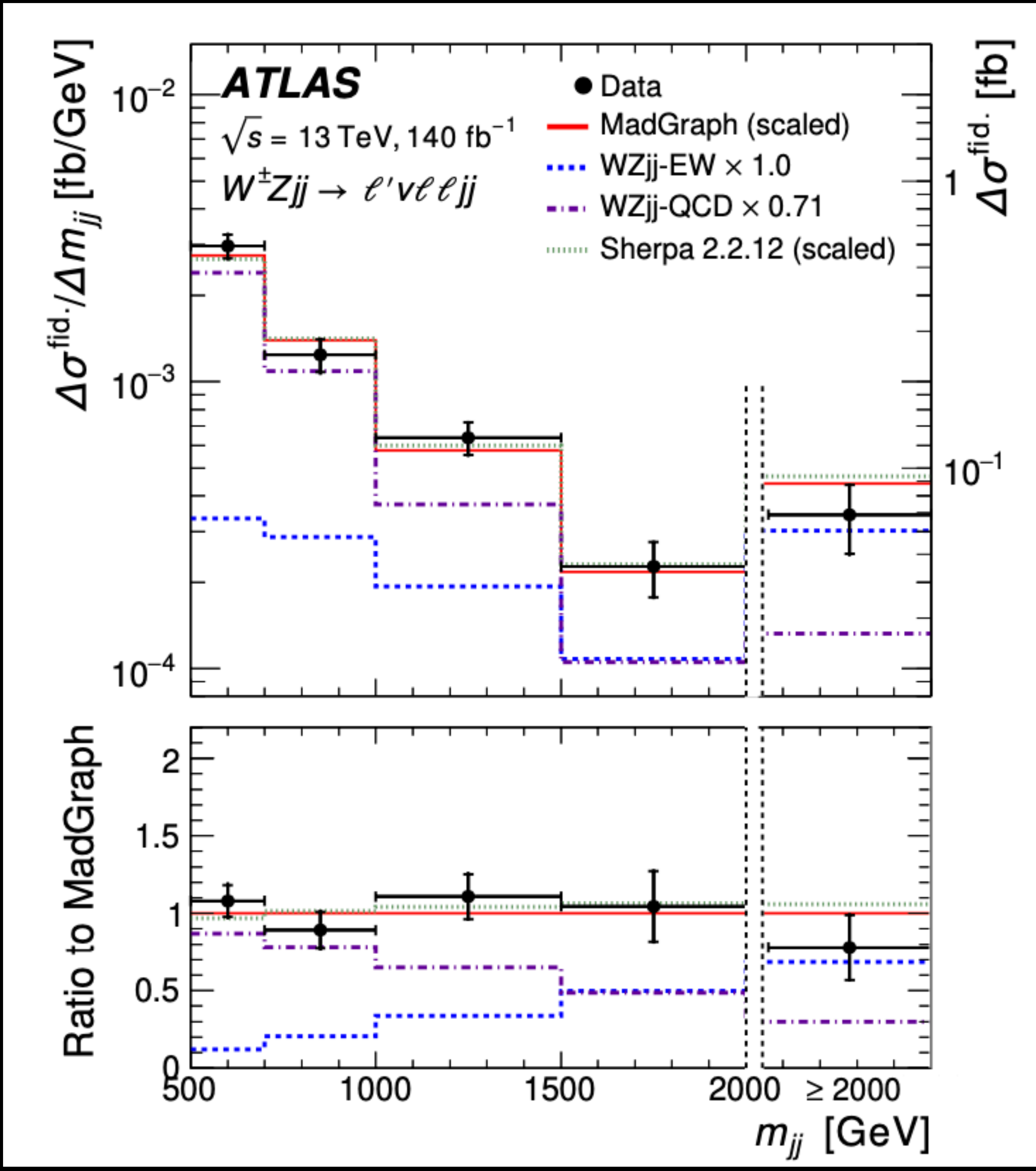

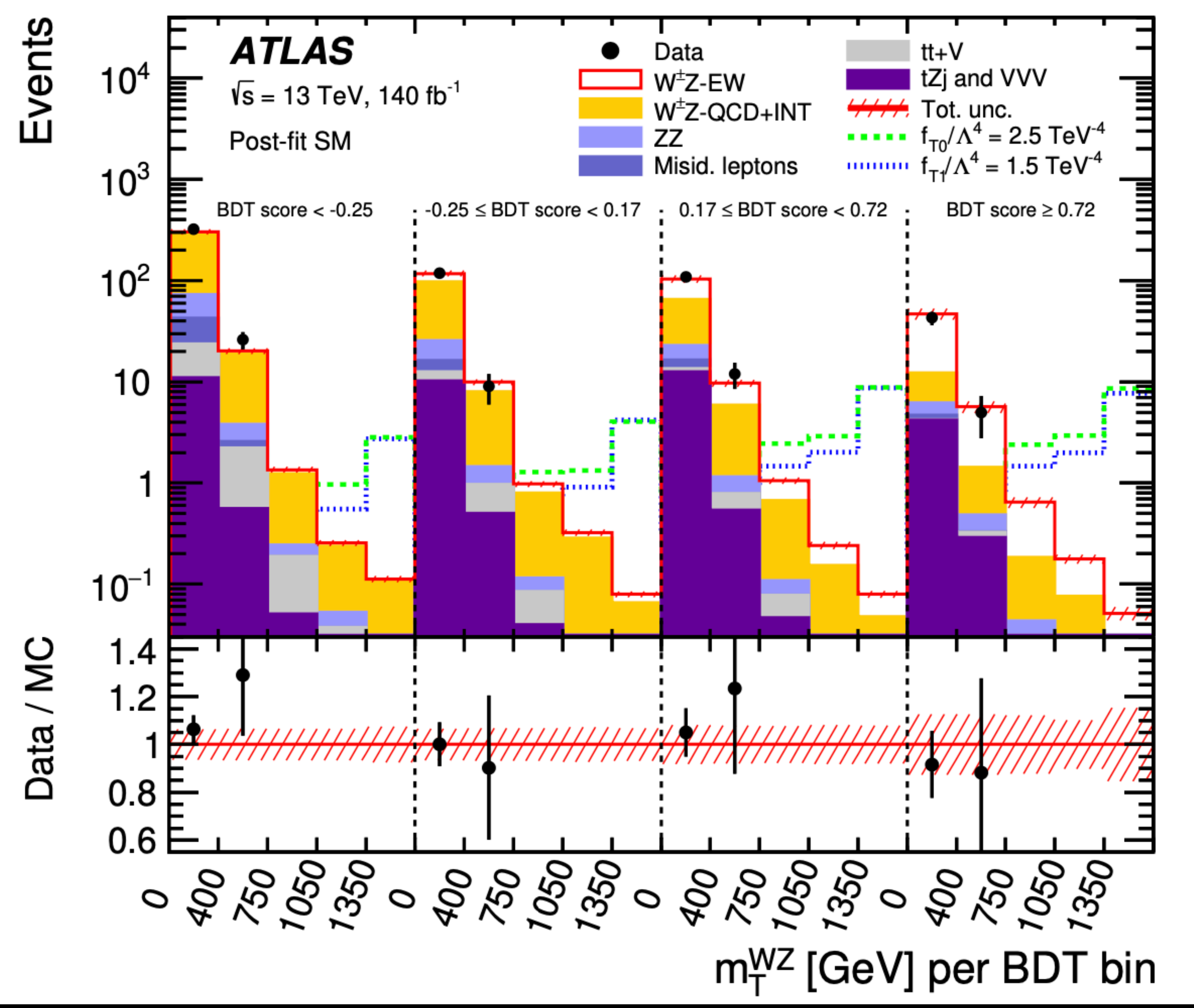

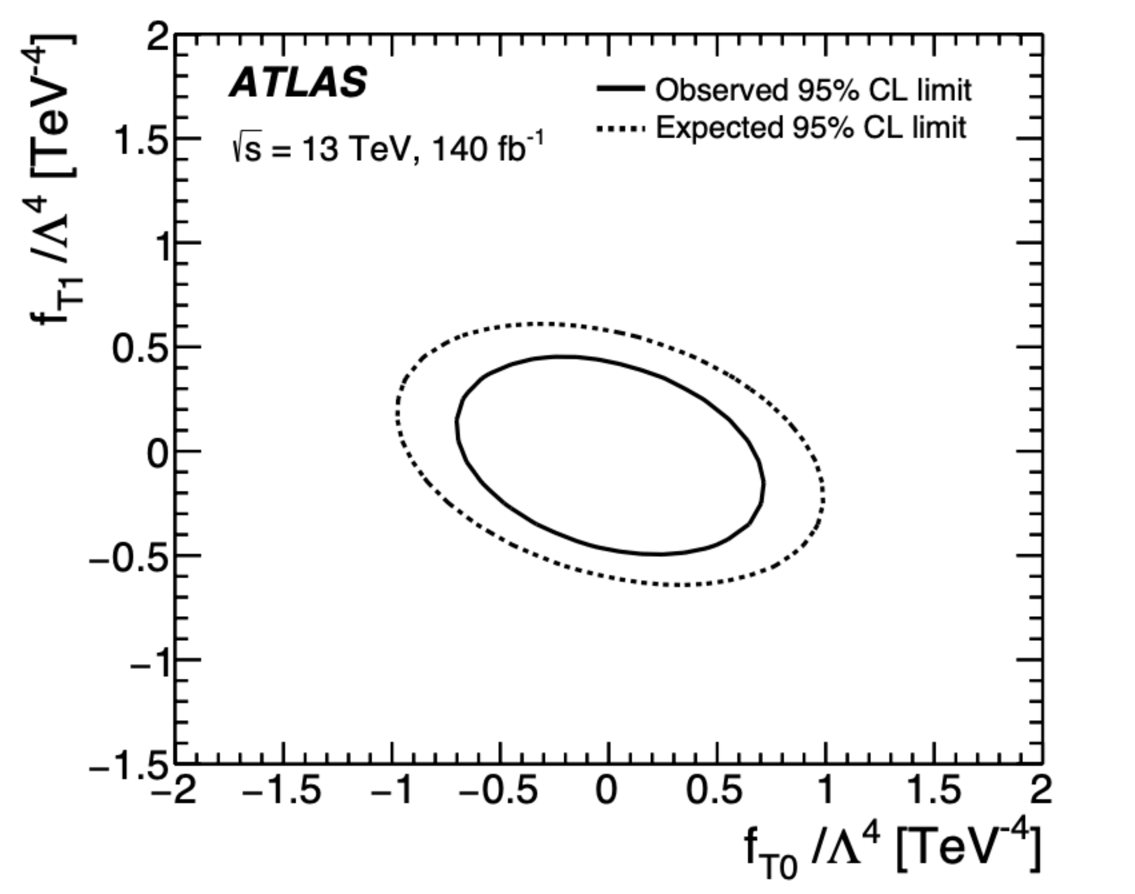

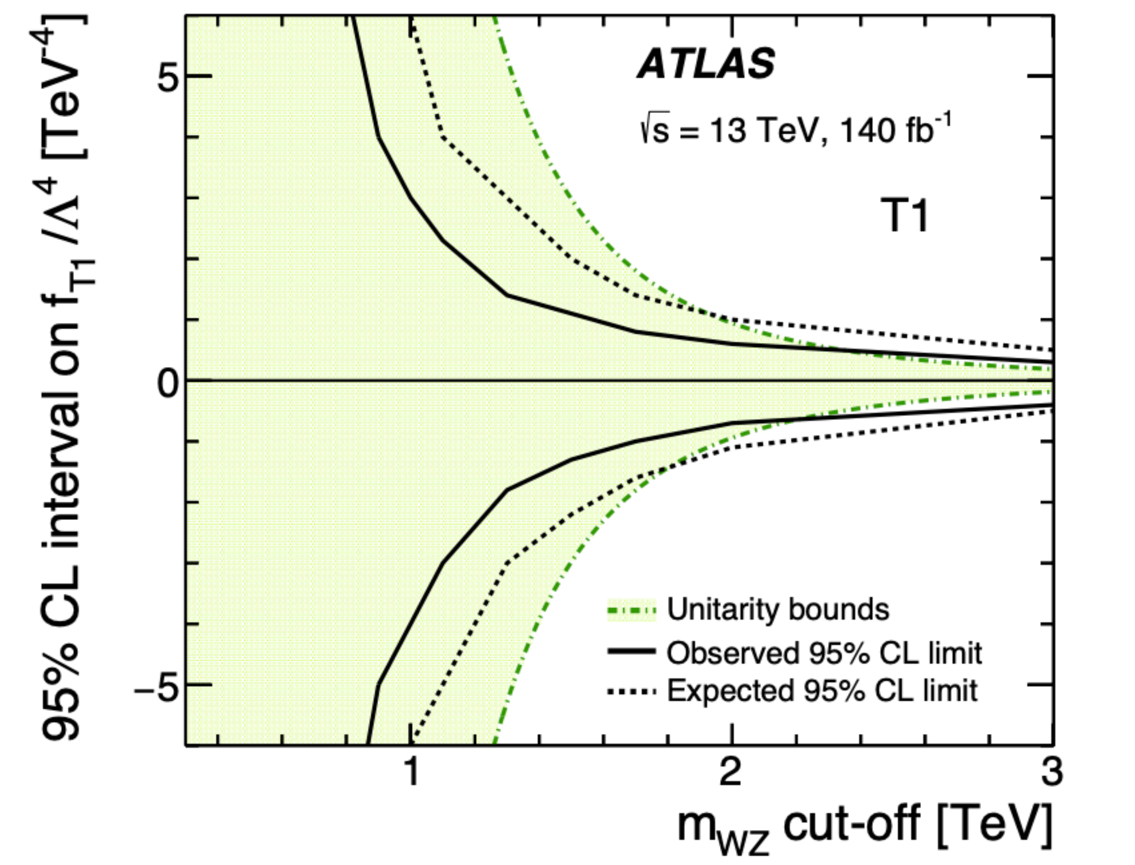

f_1/Λ^4:

Observed: [-0.39, 0.35], [-0.7, 0.6] TeV^{-4}

Expected: [-0.52, 0.49], [-1.1, 1.0] TeV^{-4}

Differential cross section in VBS fiducial region

$$c_\alpha = f_\alpha^{(8)}/\Lambda^4$$

$$\left|A_{\text{SM}} + \sum_\alpha c_\alpha A_\alpha^{(8)}\right|^2 = |A_{\text{SM}}|^2 + \sum_\alpha c_\alpha 2\mathcal{R}e(A_{\text{SM}}^* A_\alpha^{(8)}) + \sum_\alpha c_\alpha^2 |A_\alpha^{(8)}|^2 + \sum_{\alpha,\beta} c_\alpha c_\beta 2\mathcal{R}e(A_\alpha^{(8)} A_\beta^{*(8)})$$

VBS Same Sign WW with hadronic τ

http://cds.cern.ch/record/2867989?ln=en

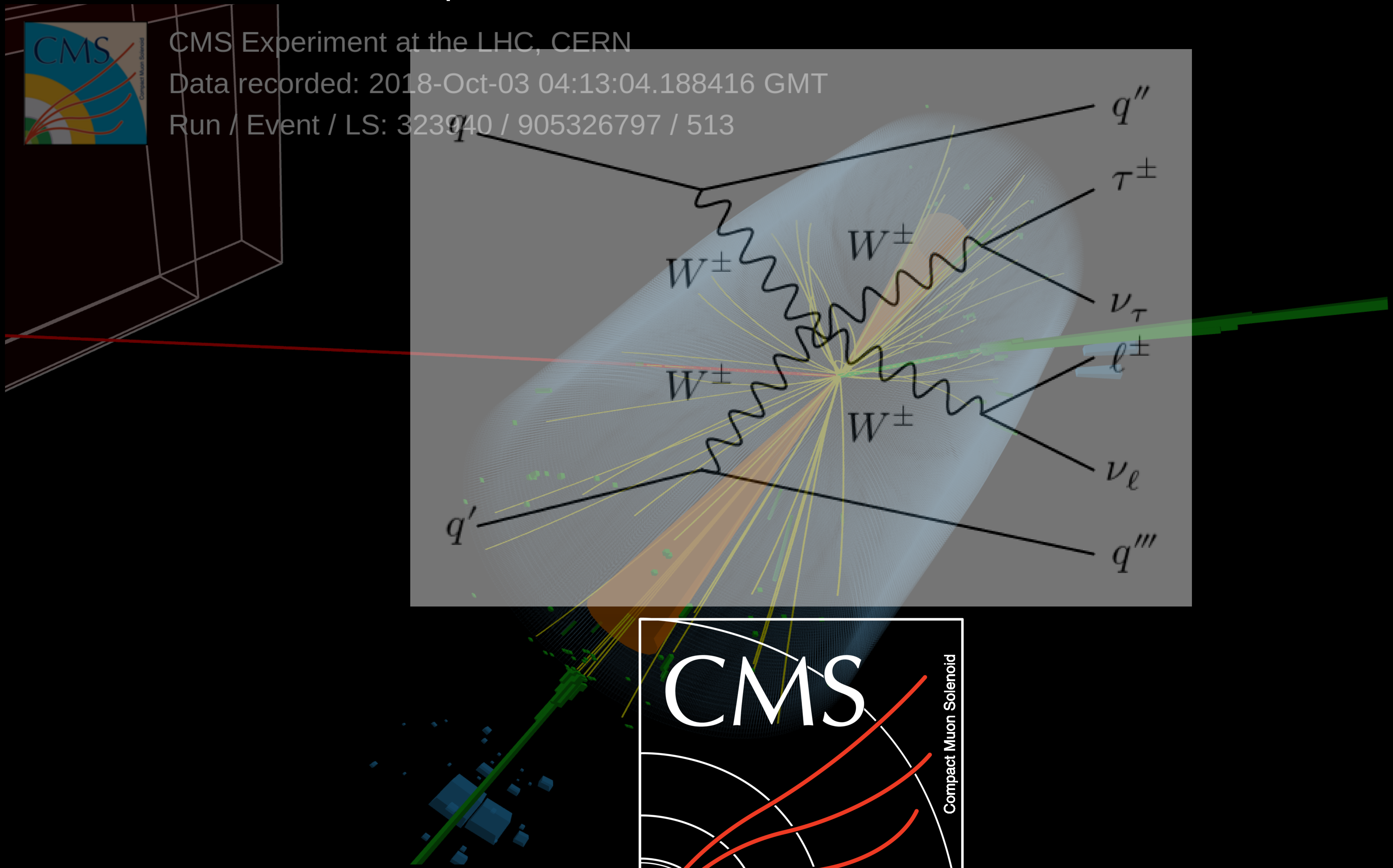

http://cds.cern.ch/record/2867989?ln=en

VBS Same Sign WW with hadronic τ

- Final state where one of the two same-signed W-bosons decays to a hadronic τ
  - Signature: $\tau_h \nu_\tau \ell \nu_\ell (\ell = e, \mu)$
- Significance of SM process at 2.7 σ, signal strength: $1.44^{+0.63}_{-0.56}$
  - Public since August 2023

$$N \propto |\mathcal{A}|^2 = |\mathcal{A}_{SM}|^2 + \sum_\alpha \frac{C_\alpha}{\Lambda^2}.2\mathcal{R}e(\mathcal{A}_{SM}\mathcal{A}_{Q\alpha}^{(6)\dagger}) + \sum_{\alpha,\beta} \frac{C_\alpha C_\beta}{\Lambda^4}.(\mathcal{A}_{Q\alpha}^{(6)}\mathcal{A}_{Q\beta}^{(6)\dagger}) +$$

Dim6 including linear, BSM and mixed contributions

$$\sum_k \left[\frac{f_k}{\Lambda^4}.2\mathcal{R}e(\mathcal{A}_{SM}\mathcal{A}_{Qk}^{(8)\dagger})\right] + \sum_k \frac{f_k^2}{\Lambda^8}.(\mathcal{A}_{Qk}^{(8)}\mathcal{A}_{Qk}^{(8)\dagger})$$

Dim8 including linear and BSM contributions

- First simultaneous extraction of dim-6 and dim-8 constraints
- Transverse mass (M_{01}) used as the variable of interest for 2D constraints

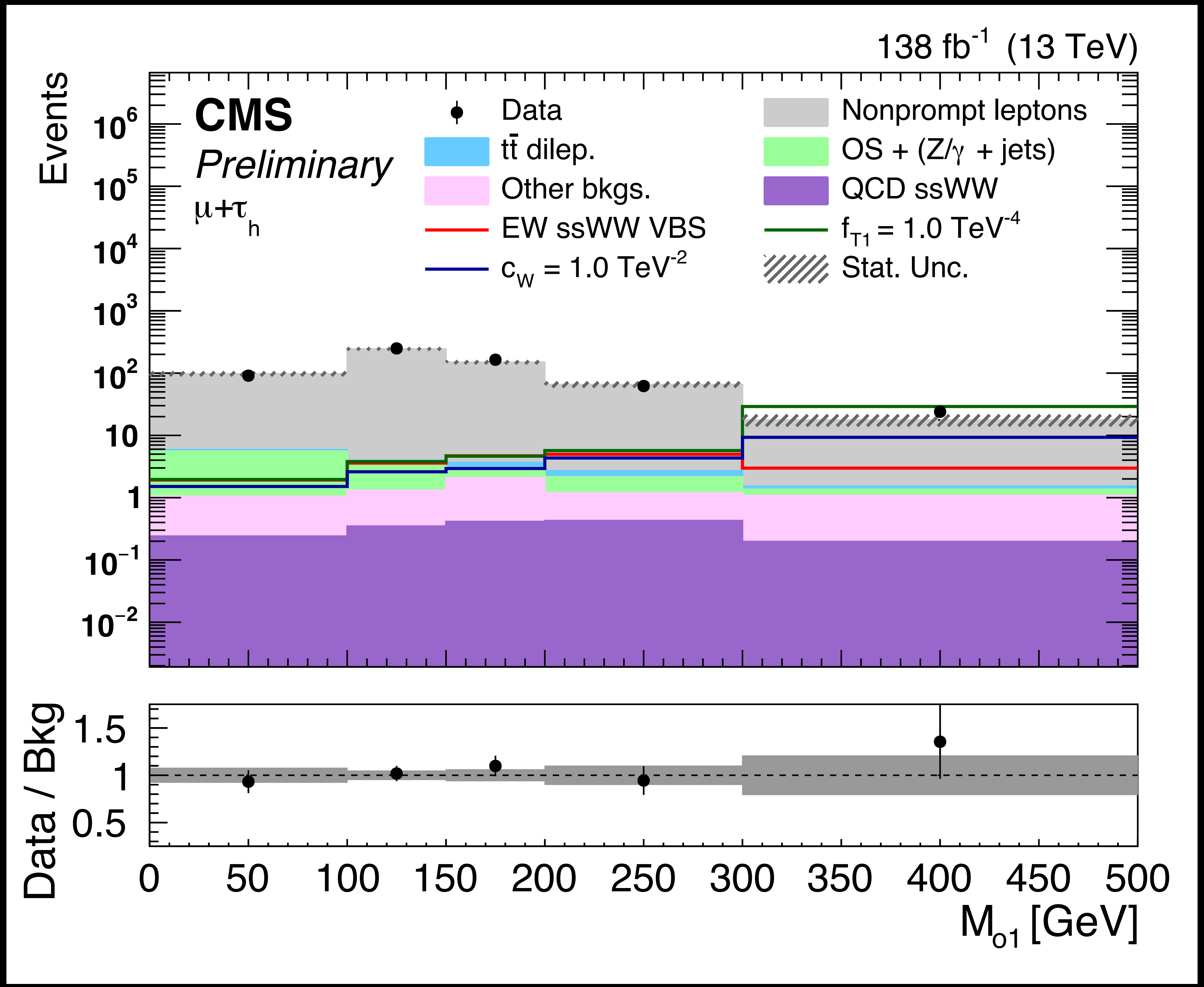

$$M_{01} = (p_{T\tau} + p_l + \vec{p}_T^{\,miss})^2 + |p_{T\tau} + \vec{p}_T^{\,miss}|^2$$

http://cds.cern.ch/record/2867989?ln=en

VBS Same Sign WW with hadronic τ

- Deep Neural Network (DNNs) trained with used to gain sensitivity to BSM signals

extracted with dim-6 DNN output distributions

extracted with dim-8 DNN output distributions

	Wilson coefficient	68% CL interval(s) Expected	68% CL interval(s) Observed	95% CL interval Expected	95% CL interval Observed
dim-6	$c_{ll}^{(1)}$	$[-12.9, -8.03] \cup [-2.95, 1.91]$	$[-11.6, 0.045]$	$[-14.6, 3.53]$	$[-13.5, 2.11]$
	$c_{qq}^{(1)}$	$[-0.501, 0.576]$	$[-0.341, 0.416]$	$[-0.742, 0.818]$	$[-0.605, 0.681]$
	c_W	$[-0.681, 0.669]$	$[-0.513, 0.481]$	$[-0.987, 0.974]$	$[-0.842, 0.818]$
	c_{HW}	$[-7.00, 6.09]$	$[-5.48, 4.31]$	$[-9.99, 9.05]$	$[-8.68, 7.60]$
	c_{HWB}	$[-41.7, 69.6]$	$[30.7, 89.2]$	$[-66.6, 96.4]$	$[-49.7, 110]$
	c_H	$[-16.6, 18.1]$	$[-12.0, 14.0]$	$[-24.7, 26.3]$	$[-20.9, 22.7]$
	c_{HD}	$[-24.6, 34.7]$	$[-15.3, 31.5]$	$[-38.2, 48.8]$	$[-31.4, 45.5]$
	$c_{Hl}^{(1)}$	$[-28.8, 29.9]$	$[-38.2, 39.5]$	$[-49.4, 49.7]$	$[-69.3, 68.3]$
	$c_{Hl}^{(3)}$	$[-1.43, 2.23] \cup [5.88, 9.54]$	$[-0.045, 8.58]$	$[-2.64, 10.8]$	$[-1.59, 9.94]$
	$c_{Hq}^{(1)}$	$[-4.53, 4.42]$	$[-3.27, 3.44]$	$[-6.56, 6.44]$	$[-5.55, 5.60]$
	$c_{Hq}^{(3)}$	$[-2.39, 1.37]$	$[-1.88, 0.705]$	$[-3.24, 2.16]$	$[-2.82, 1.61]$
dim-8	f_{T0}	$[-1.02, 1.08]$	$[-0.774, 0.842]$	$[-1.52, 1.58]$	$[-1.32, 1.38]$
	f_{T1}	$[-0.426, 0.480]$	$[-0.319, 0.381]$	$[-0.640, 0.695]$	$[-0.552, 0.613]$
	f_{T2}	$[-1.15, 1.37]$	$[-0.851, 1.12]$	$[-1.75, 1.98]$	$[-1.51, 1.76]$
	f_{M0}	$[-9.89, 9.74]$	$[-8.07, 7.70]$	$[-14.6, 14.5]$	$[-13.1, 12.8]$
	f_{M1}	$[-12.5, 13.3]$	$[-9.54, 11.15]$	$[-18.7, 19.6]$	$[-16.4, 17.7]$
	f_{M7}	$[-20.3, 19.2]$	$[-17.6, 15.3]$	$[-29.9, 28.8]$	$[-27.6, 25.8]$
	f_{S0}	$[-11.6, 12.0]$	$[-9.60, 9.82]$	$[-17.4, 17.9]$	$[-15.9, 16.1]$
	f_{S1}	$[-37.4, 38.8]$	$[-40.9, 41.3]$	$[-57.2, 58.6]$	$[-60.9, 61.8]$
	f_{S2}	$[-37.4, 38.8]$	$[-40.9, 41.3]$	$[-57.2, 58.6]$	$[-60.9, 61.8]$

http://cds.cern.ch/record/2867989?ln=en

VBS Same Sign WW with hadronic τ

$$M_{01} = (p_{T\tau} + p_l + \overrightarrow{p}_T^{miss})^2 + |p_{T\tau} + \overrightarrow{p}_T^{miss}|^2$$

- Simultaneous extraction of dim-6 and dim-8 constraints

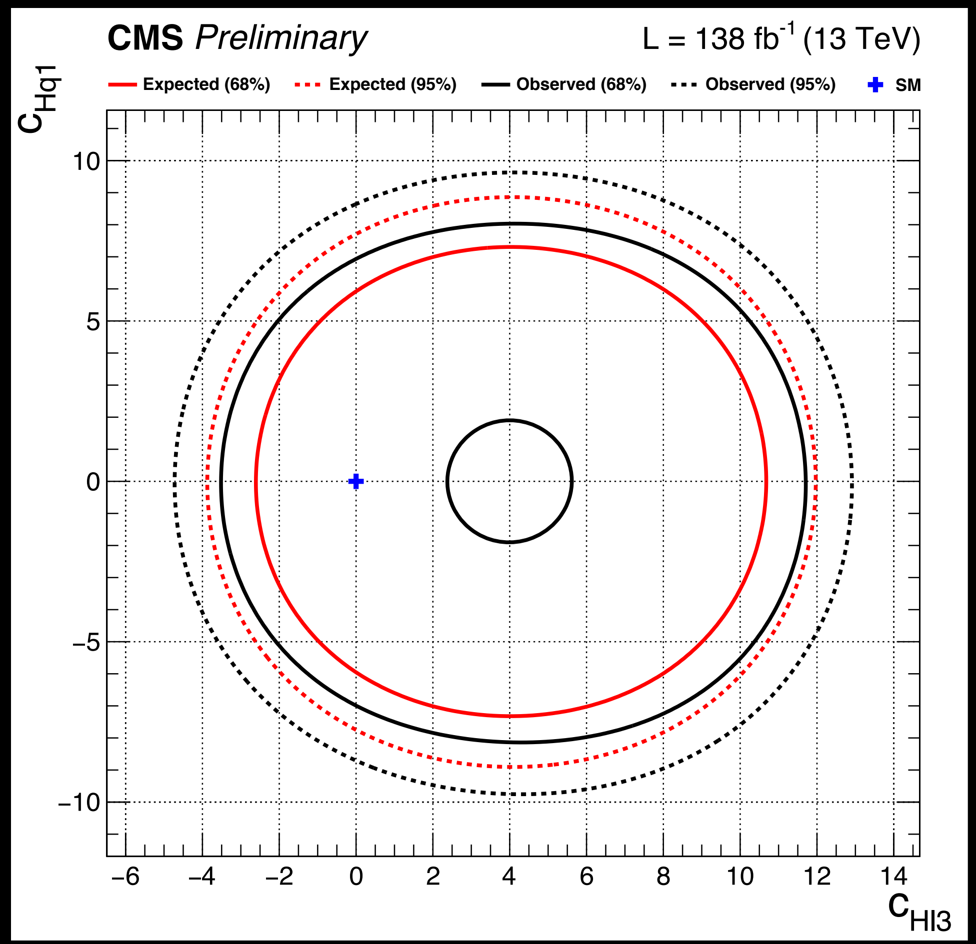

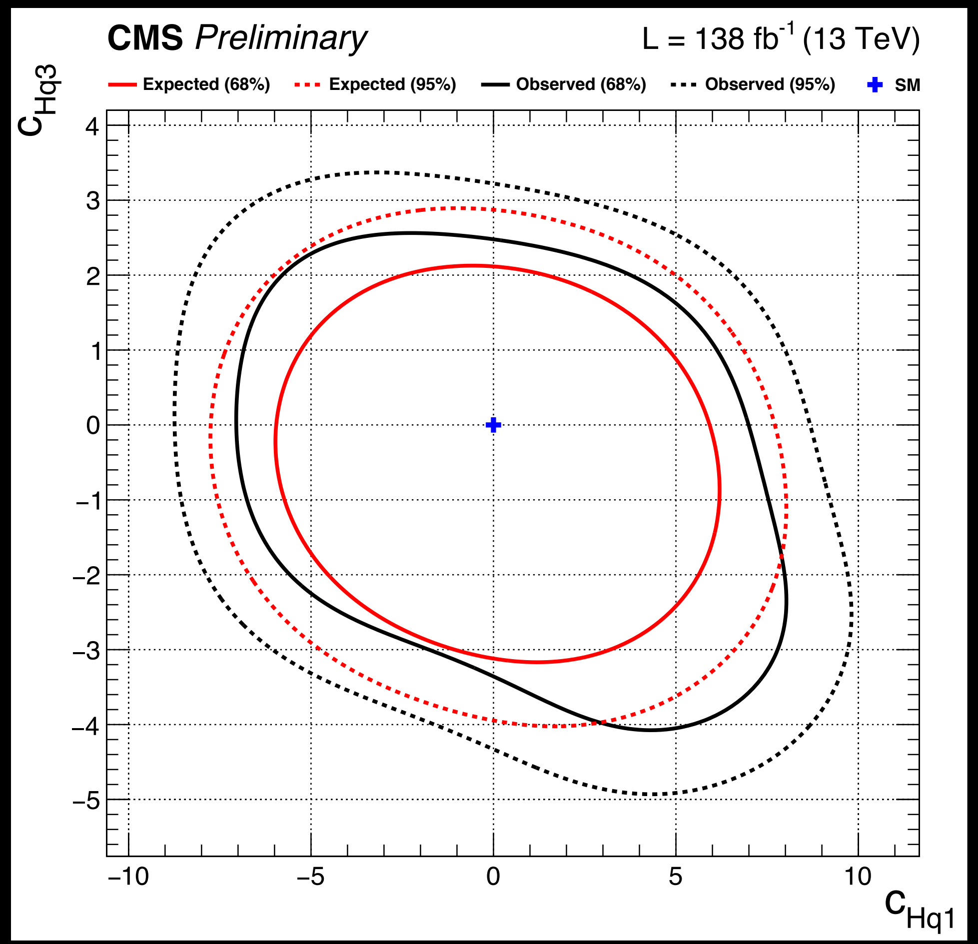

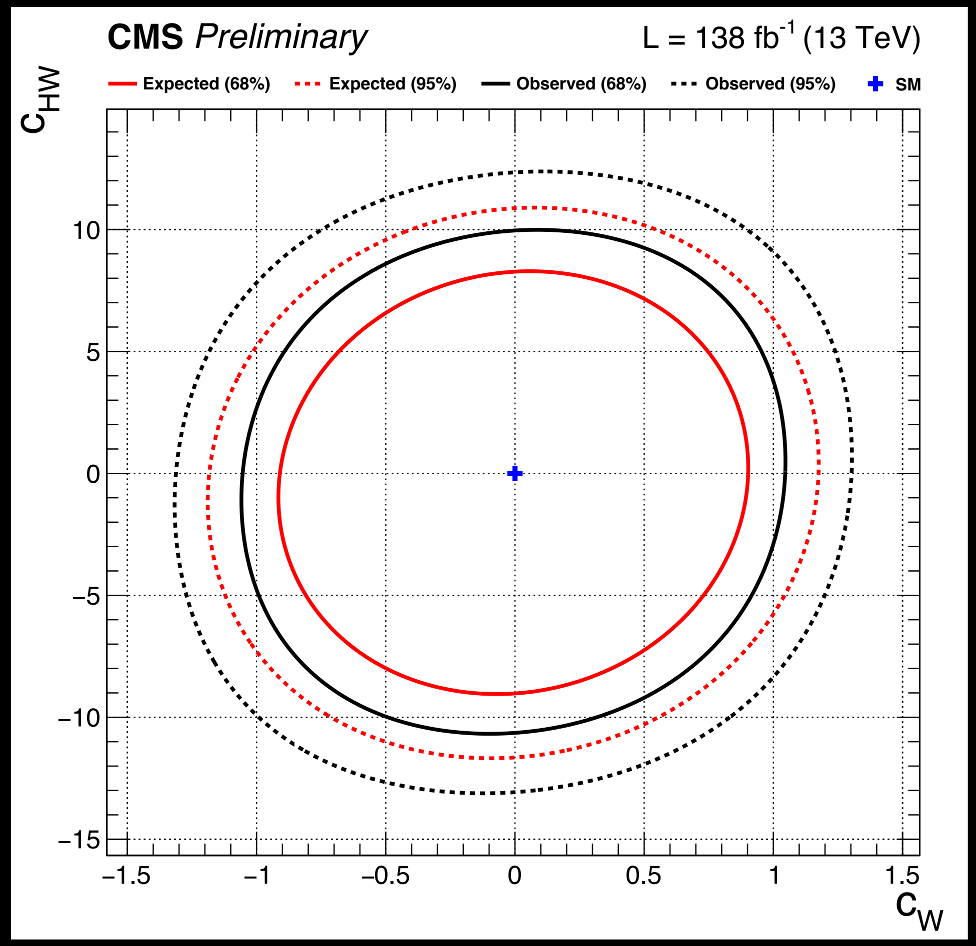

Sensitive to correlation between Higgs-fermion operators

Fits between boson operators of dim-6 and dim-8

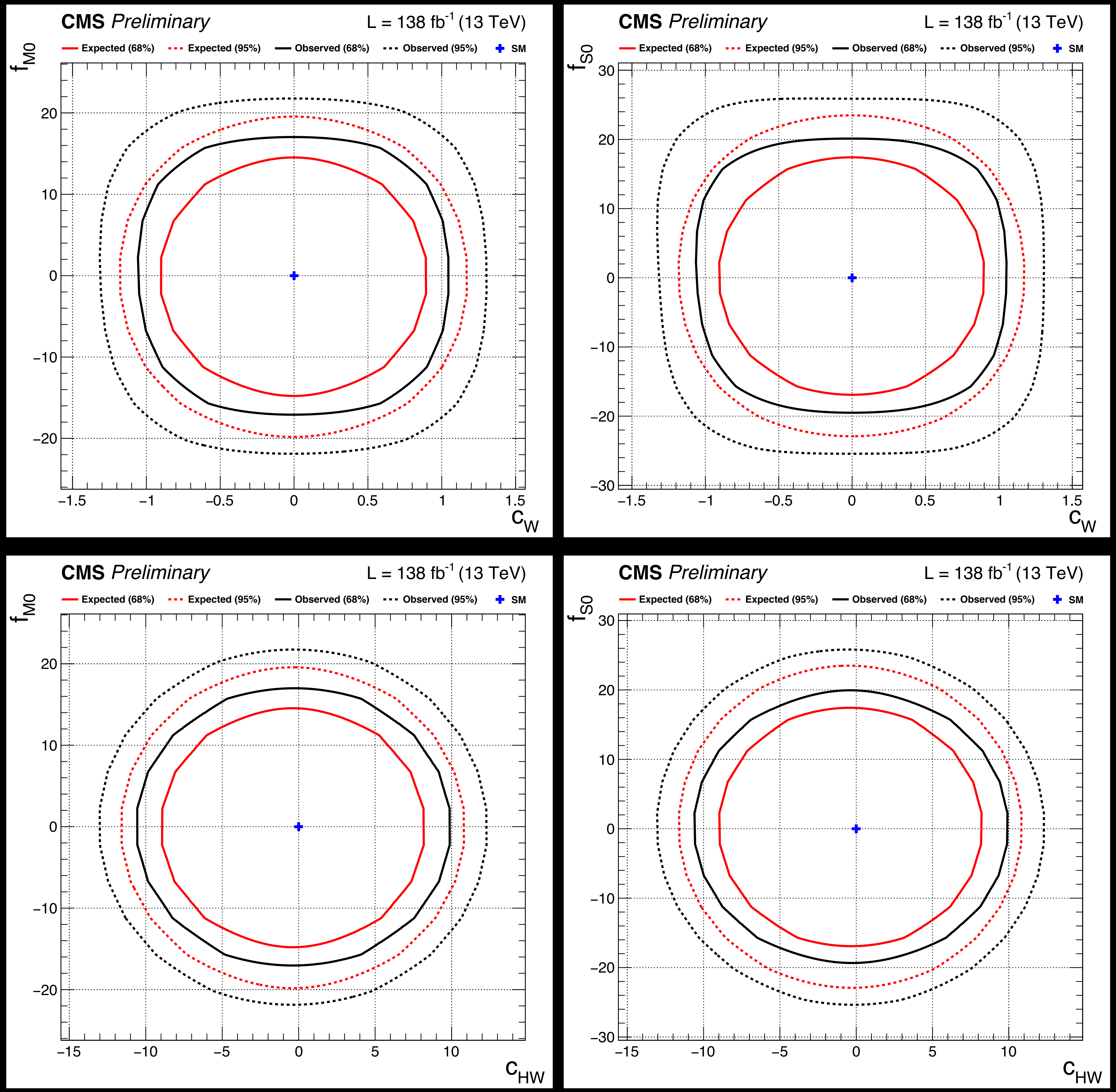

Polarization — energy dependence and the Radiation Amplitude Zero effect

https://arxiv.org/abs/2402.16365

ATLAS EXPERIMENT

https://arxiv.org/abs/2402.16365

Polarization measurement in WZ process

- Study of different polarization states in diboson processes → sensitive probe of electroweak symmetry breaking
- Boosted decision tree trained to measure polarization fractions (7 variables):
  - f_{00} (f_{TT}) both bosons longitudinally (transversely) polarized
  - f_{0T} (f_{T0}): $W(Z)$ boson is longitudinally polarized, $Z(W)$ is transversely polarized
  - New: measurement of fractions in high p_T^Z regime and low p_T^{WZ}
    - Leads to an improvement of 20-30% in f_{00}

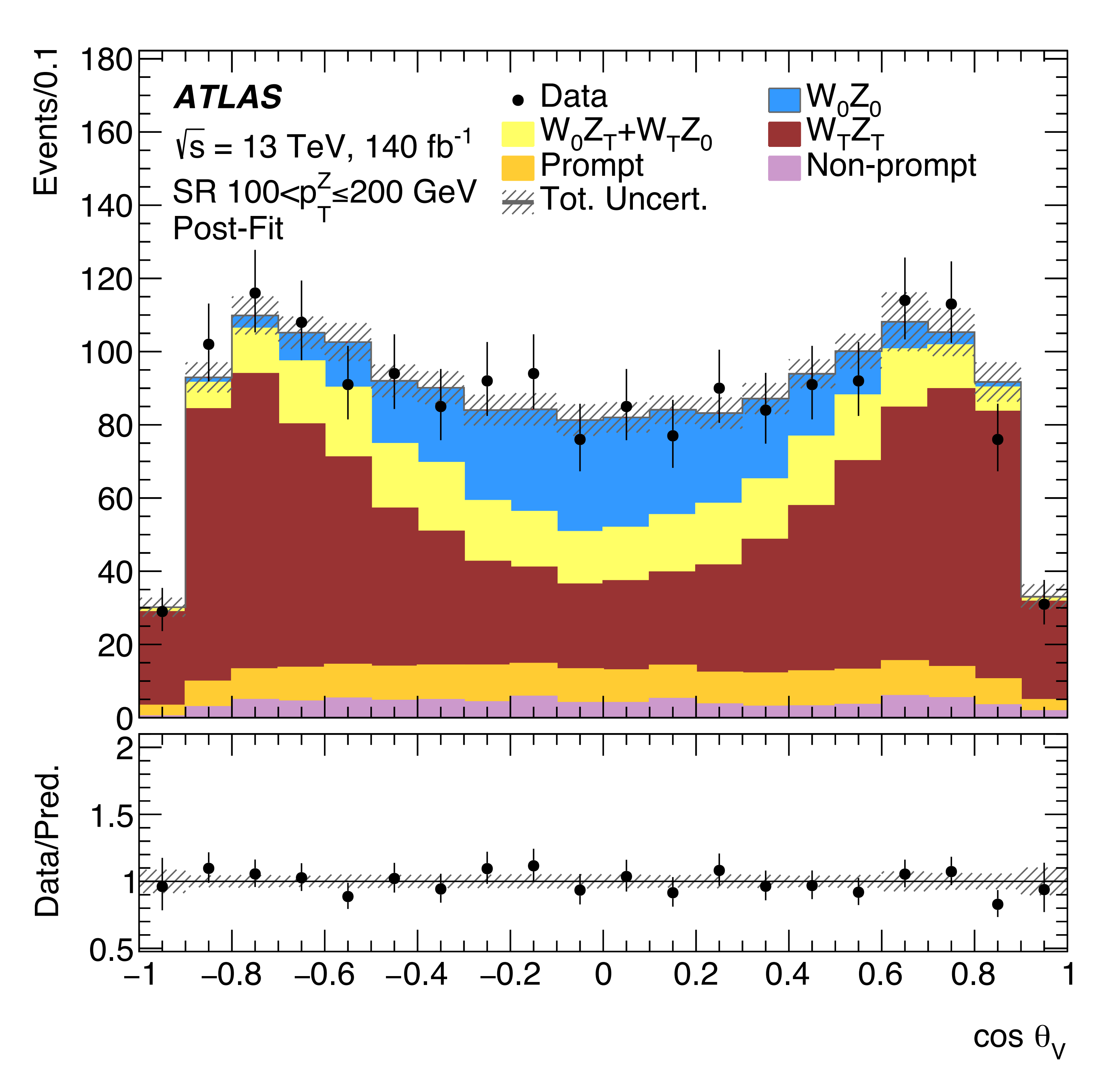

θ_V : scattering angle of the W boson in the WZ rest frame with respect to the z-axis

	Measurement		Prediction		
	$100 < p_T^Z \leq 200$ GeV	$p_T^Z > 200$ GeV		$100 < p_T^Z \leq 200$ GeV	$p_T^Z > 200$ GeV
f_{00}	$0.19 \pm^{0.03}_{0.03}$ (stat) $\pm^{0.02}_{0.02}$ (syst)	$0.13 \pm^{0.09}_{0.08}$ (stat) $\pm^{0.02}_{0.02}$ (syst)	f_{00}	0.152 ± 0.006	0.234 ± 0.007
f_{0T+T0}	$0.18 \pm^{0.07}_{0.08}$ (stat) $\pm^{0.05}_{0.06}$ (syst)	$0.23 \pm^{0.17}_{0.18}$ (stat) $\pm^{0.06}_{0.10}$ (syst)	f_{0T}	0.120 ± 0.002	0.062 ± 0.002
f_{TT}	$0.63 \pm^{0.05}_{0.05}$ (stat) $\pm^{0.04}_{0.04}$ (syst)	$0.64 \pm^{0.12}_{0.12}$ (stat) $\pm^{0.06}_{0.06}$ (syst)	f_{T0}	0.109 ± 0.001	0.058 ± 0.001
f_{00} obs (exp) sig.	5.2 (4.3) σ	1.6 (2.5) σ	f_{TT}	0.619 ± 0.007	0.646 ± 0.008

Fraction of events where both bosons are longitudinally polarized measured with an observed significance of 5.2 σ (1.6 σ) in the phase space: $100 < p_T^Z < 200$ GeV ($p_T^Z > 200$ GeV)

https://arxiv.org/abs/2402.16365

Radiation Amplitude Zero effect in WZ at 13 TeV

- Dominant helicity amplitude with two transversely-polarized bosons exactly zero
  - when scattering angle of the W boson in the WZ rest frame (w.r.t the incoming antiquark direction) approaches 90^0 → Radiation Amplitude Zero (RAZ)
  - arises from the gauge structure in the SM
- RAZ ⇒ drop at 0 in the $\Delta Y(WZ)$ (rapidity difference between W and Z bosons) and $\Delta Y(l_W Z)$ (rapidity difference between lepton from W decay and Z boson) distributions
- First observation of RAZ effect in WZ production, seen in $W\gamma$ previously (SMP-20-005), longitudinally polarized $W's$ make observation challenging
- Next-to-leading order (NLO) QCD correction dilute the effect, hadronic activity reduced by placing stringent requirement on p_T^{WZ}

https://arxiv.org/abs/2402.16365

Radiation Amplitude Zero effect in WZ at 13 TeV

Unfolded distributions

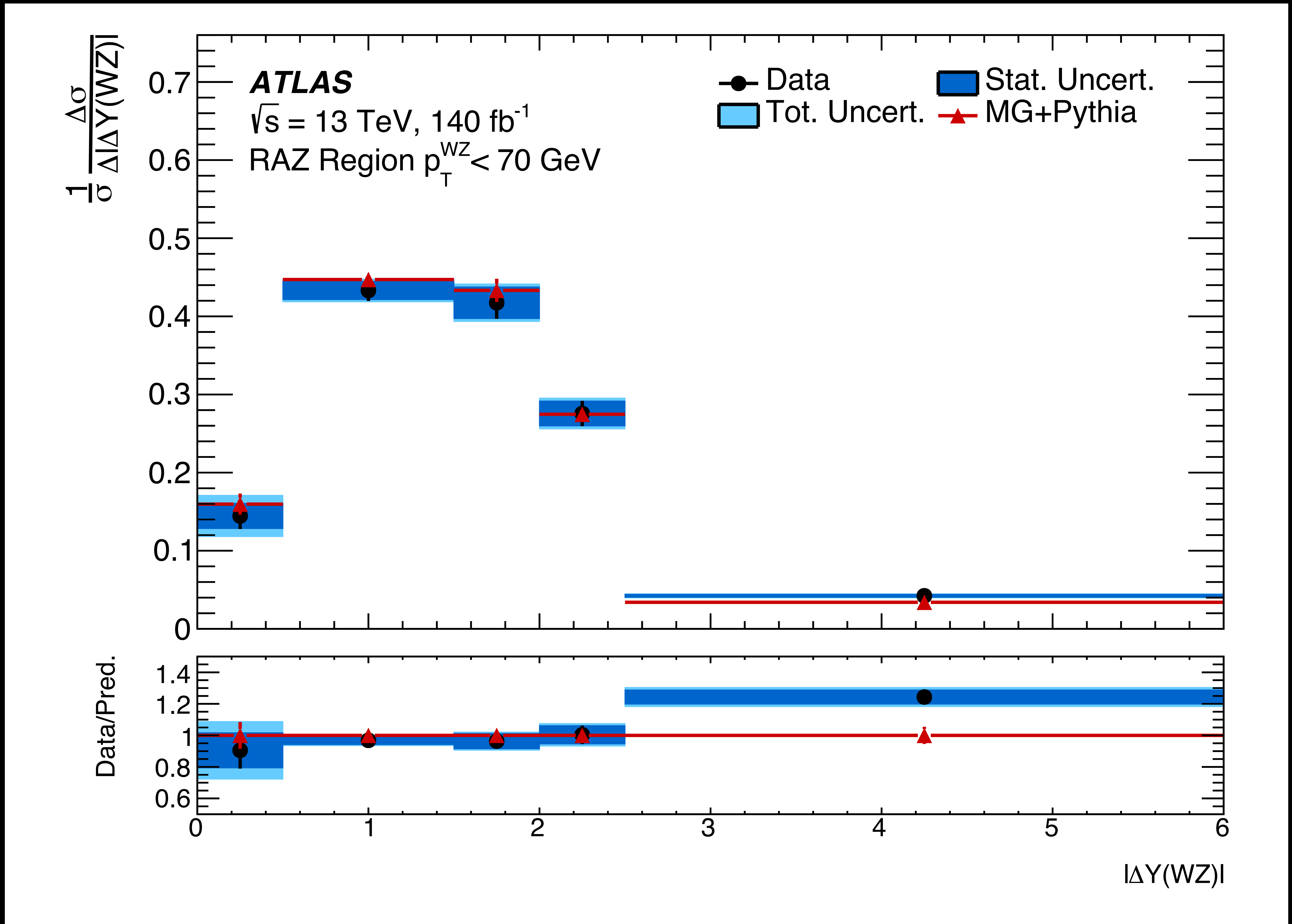

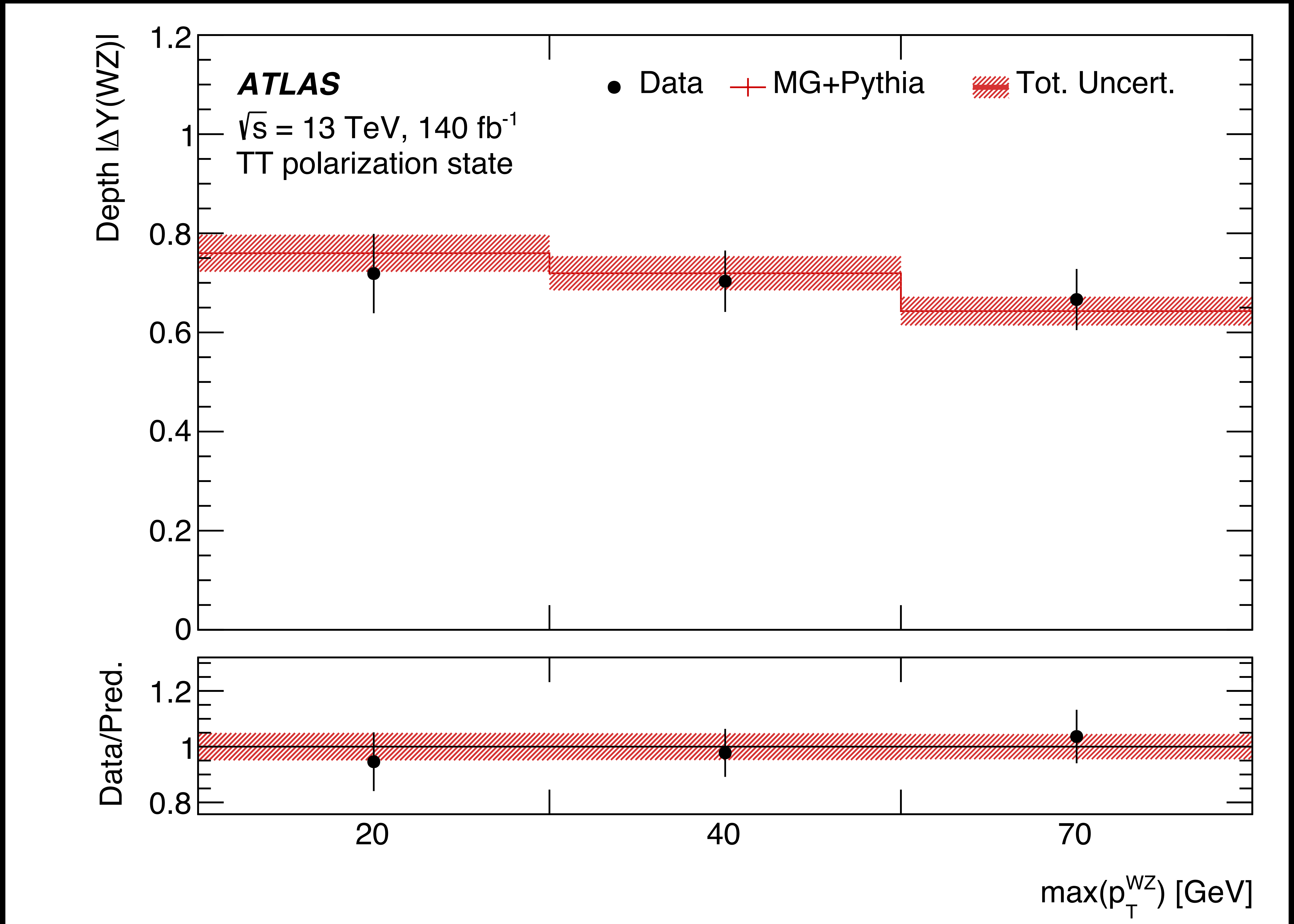

Effect expected for only transversely polarized bosons, all other polarization components are subtracted

Depth of the RAZ dip defined as

$$\mathscr{D} = 1 - 2 \times \left(\frac{N(|\Delta Y(WZ)| < 0.5)}{N(0.5 < |\Delta Y(\ell_W Z)| < 1.5)} \right), +\mathscr{D} \Rightarrow \text{dip}$$

Anomalous neutral gauge couplings in the mono photon channel

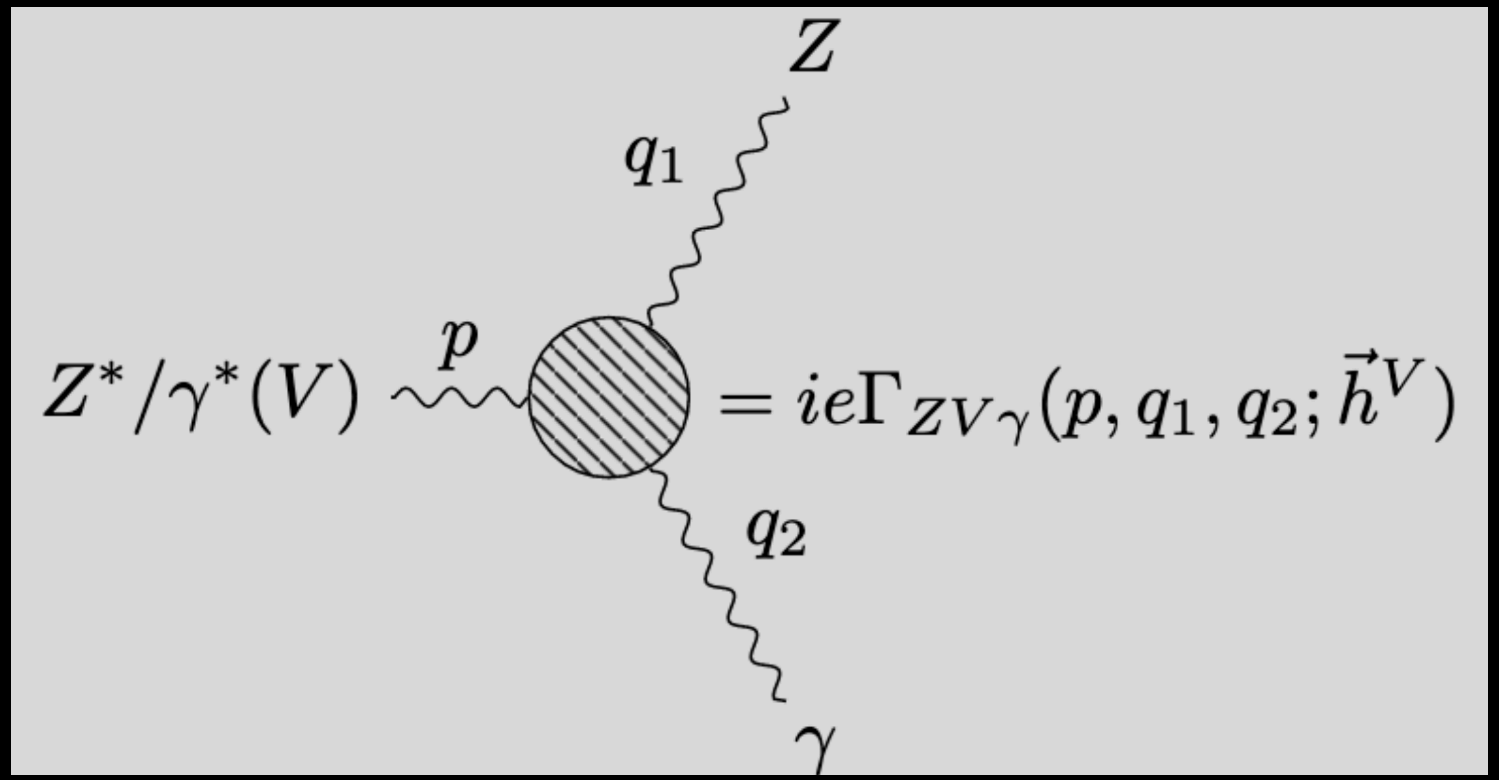

Anomalous neutral gauge couplings in the mono photon channel

- Generalized theory of forbidden neutral gauge couplings
  - Parametrized with 8 parameters (h_1 to h_4)
  - $Z + \gamma$ cross section deviation at high p_T
  - Backgrounds range from $W + \gamma$, $V + \text{jets}$, $\gamma + \text{jets}$ and dibosons estimated using data-driven methods and simulations

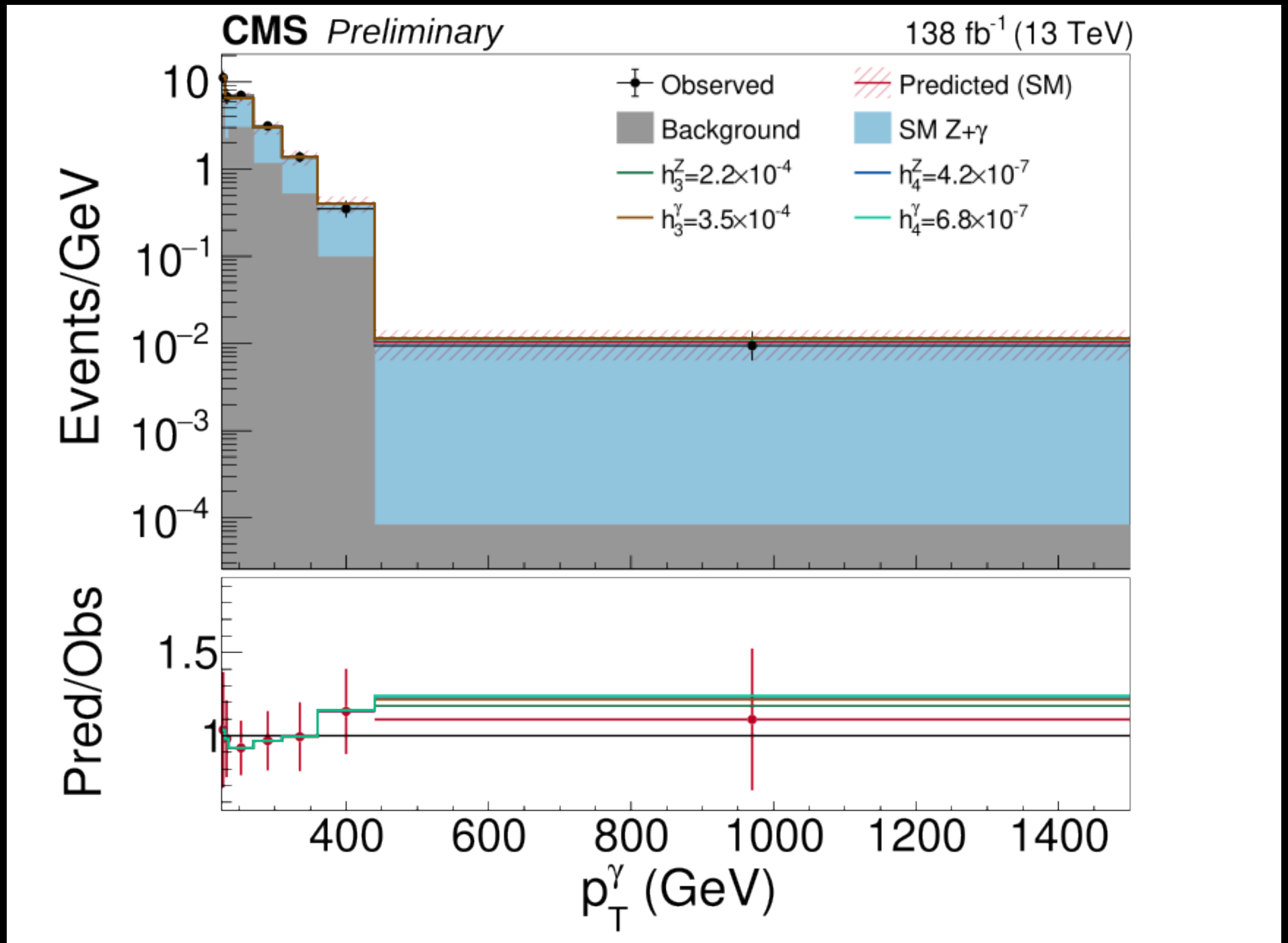

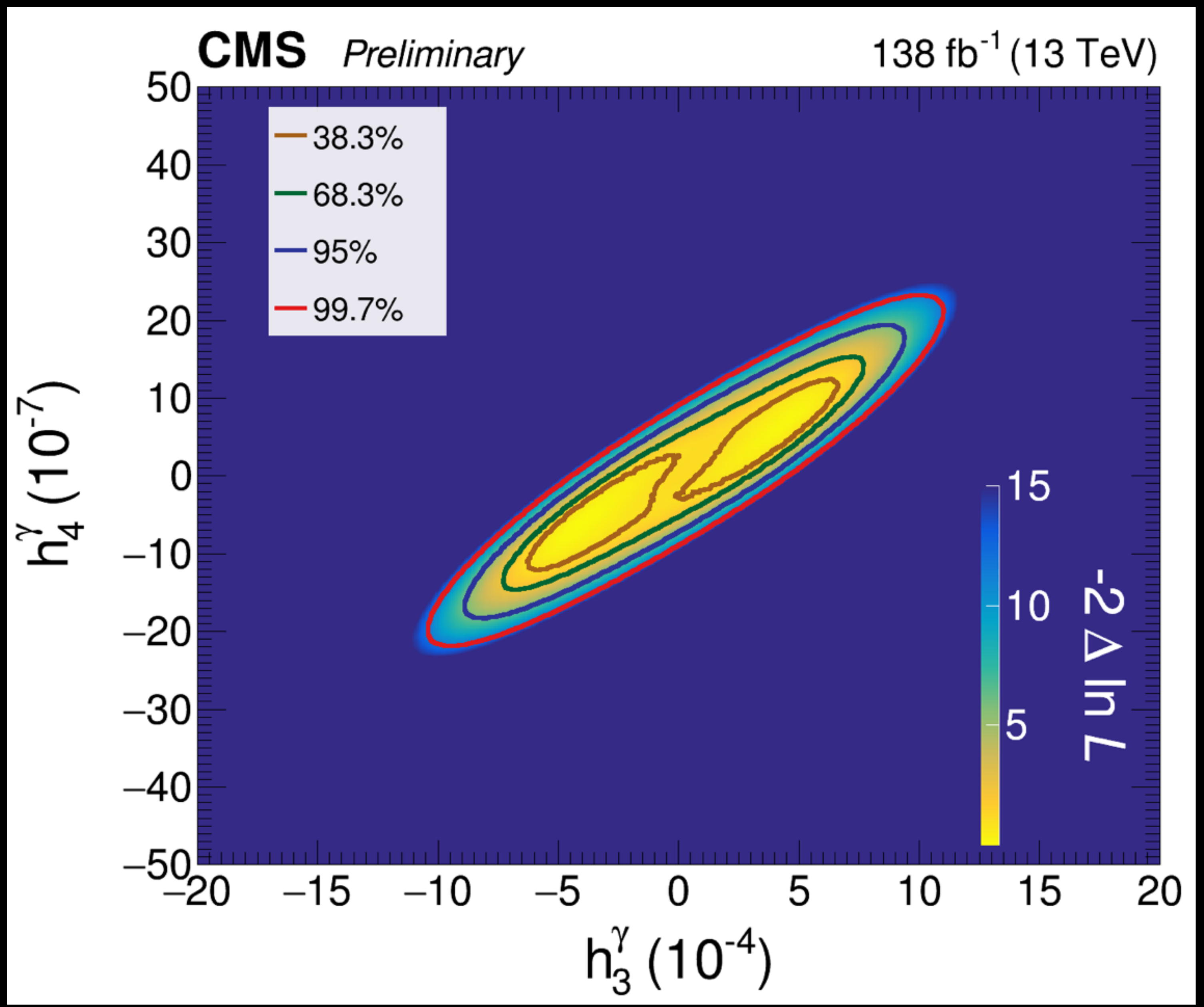

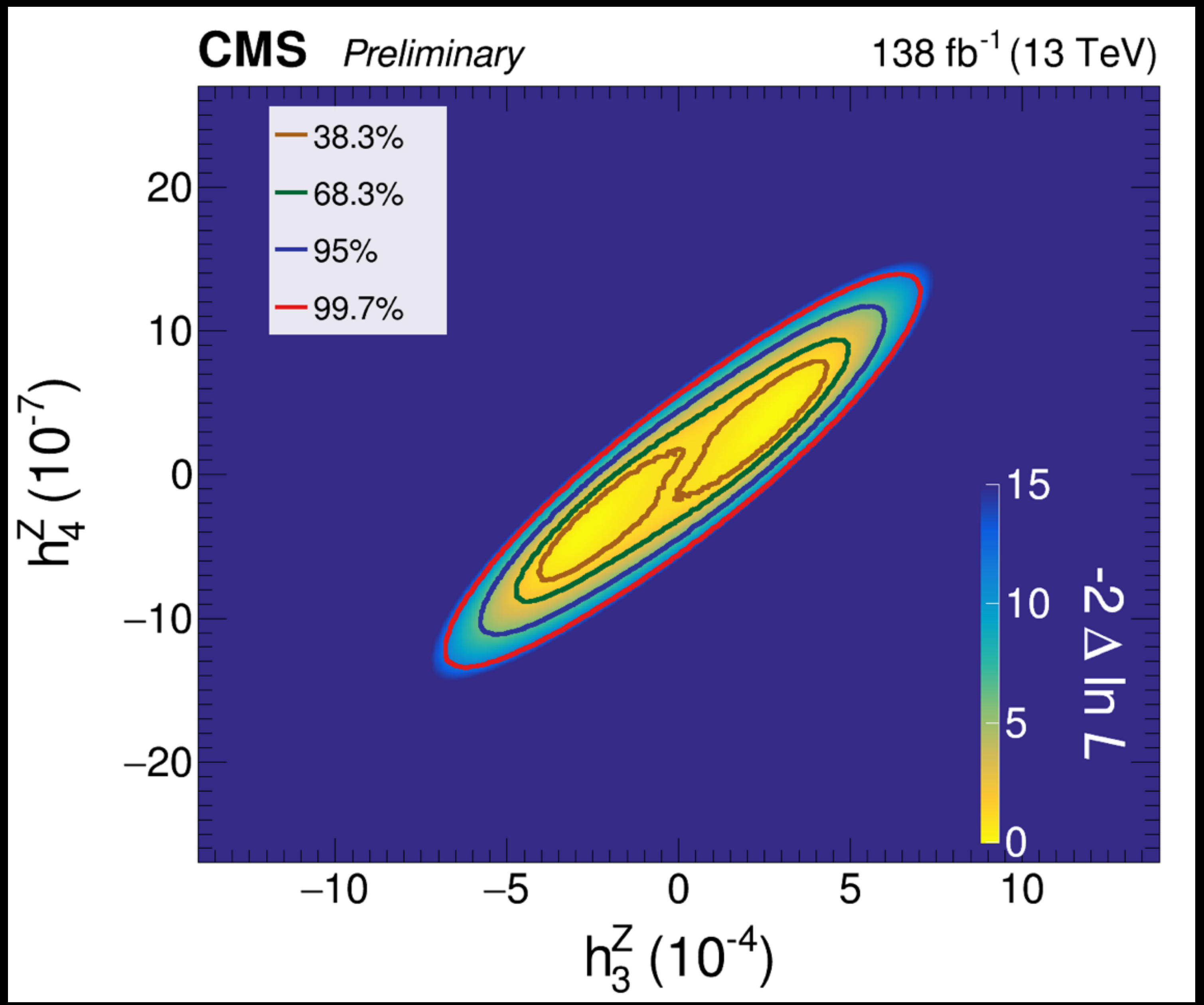

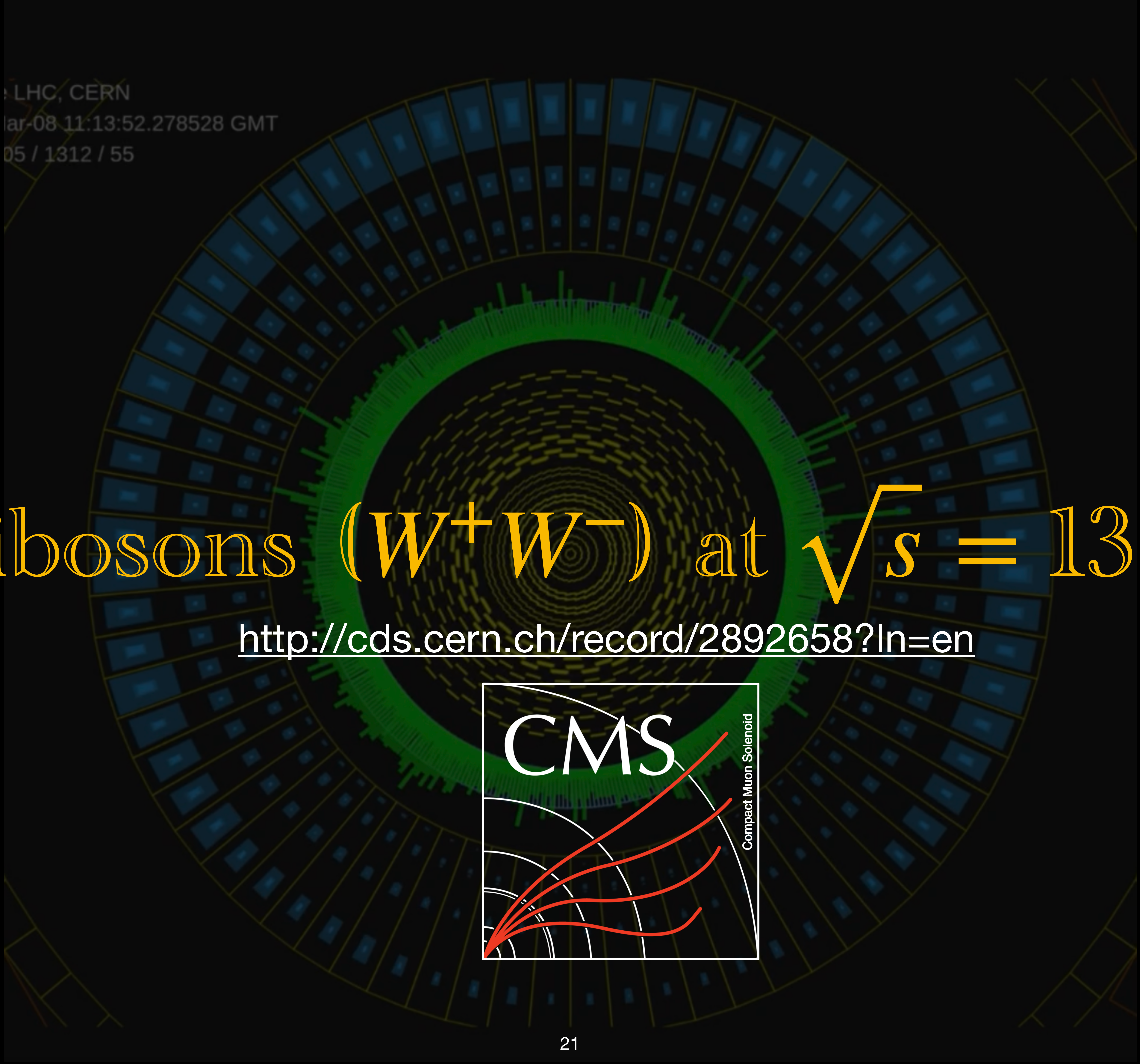

Multibosons (W^+W^-) at $\sqrt{s}$ = 13.6 TeV

http://cds.cern.ch/record/2892658?ln=en

http://cds.cern.ch/record/2892658?ln=en

W^+W^- cross section measurement at 13.6 TeV

LUM-22-001

- First measurement of W^+W^- at 13.6 TeV
- Used data collected in 2022 → 34.8 fb^{-1}
- Event category: 1 muon and 1 electron of opposite charge
- The inclusive cross section is 125.7 ± 5.6 pb, in agreement with predictions

Additional $WZ \to 3\ell\nu$ and $ZZ \to 4\ell$ control regions (CRs) defined

Quantity	WW SR	One/two b-tags CRs	$Z \to \tau\tau$ CR	Same-sign CR
Number of tight leptons	Strictly 2			
Additional loose leptons	0			
Lepton charges	Opposite			Same
$p_T^{\ell\,\max}$	> 25 GeV			
$p_T^{\ell\,\min}$	> 20 GeV			
$m_{\ell\ell}$	> 85 GeV	> 85 GeV	< 85 GeV	> 85 GeV
$p_T^{\ell\ell}$	—	—	< 30 GeV	—
Number of b-tagged jets	0	1/2	0	0
N_J	$0/1/2/\geq 3$			

http://cds.cern.ch/record/2892658?ln=en

W^+W^- cross section measurement at 13.6 TeV

LUM-22-001

- First measurement of W^+W^- at 13.6 TeV
- Used data collected in 2022 → 34.8 fb^{-1}
- Event category: 1 muon and 1 electron of opposite charge
- The inclusive cross section is 125.7 ± 5.6 pb, in agreement with predictions

Additional $WZ \to 3\ell\nu$ and $ZZ \to 4\ell$ control regions (CRs) defined

Quantity		…tags CRs	$Z \to \tau\tau$ CR	Same-sign CR
Number of tight leptons		Strictly 2		
Additional loose leptons		0		
Lepton charges		…site		Same
$p_T^{\ell\,\max}$		> 25 GeV		
$p_T^{\ell\,\min}$		> 20 GeV		
$m_{\ell\ell}$		…eV	< 85 GeV	> 85 GeV
$p_T^{\ell\ell}$			< 30 GeV	—
Number of b-tagged jets			0	0
N_J		$0/1/2/\geq 3$		

	WW SR
Data	43898
WW	16220 ± 650
Top quark	19760 ± 480
$Z \to \tau\tau$	2124 ± 72
WZ	487 ± 21
ZZ	37.1 ± 1.7
Nonprompt	4860 ± 320
VVV	75.9 ± 3.7
tVx	10.7 ± 1.5
$V\gamma$	225 ± 18
Higgs	90 ± 14
Total	43890 ± 410

http://cds.cern.ch/record/2892658?ln=en

W^+W^- cross section measurement at 13.6 TeV

- Pre-fit agreement within 10% across all regions
- Including top CR in simultaneous fit with signal leads to better control of b-tagging and jet energy scale uncertainty

http://cds.cern.ch/record/2892658?ln=en

W^+W^- cross section measurement at 13.6 TeV

Observable	Requirement
Lepton origin	Direct decay of a W boson
Lepton definition	Dressed-leptons ($e^{\pm}\mu^{\mp}$)
Leading lepton p_T	$p_T^{\ell\,max} > 25\,GeV$
Trailing lepton p_T	$p_T^{\ell\,min} > 20\,GeV$
$\lvert\eta\rvert$ of leptons	$\lvert\eta\rvert < 2.5$
Dilepton mass	$m_{\ell\ell} > 85\,GeV$
Jet p_T	$p_T^{j} > 30\,GeV$
$\lvert\eta\rvert$ of jets	$\lvert\eta^{j}\rvert < 2.5$
Jet-lepton removal	$\Delta R(j, \ell) > 0.4$

- First comparison of normalized fiducial cross section for the W^+W^- process using MiNNLOPS
- Excellent agreement between data and prediction in all jet bins

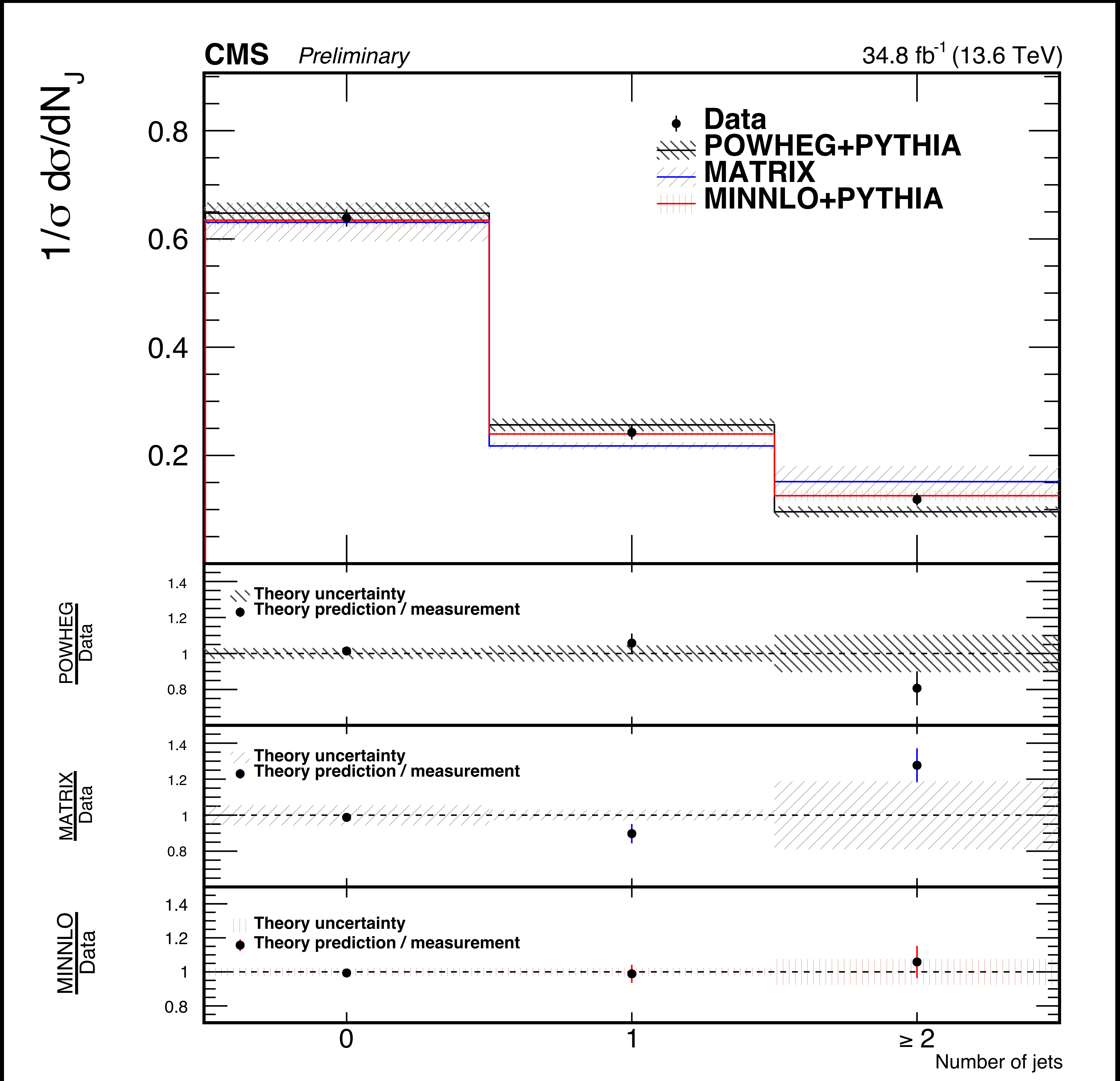

Many analyses performed and more to come…

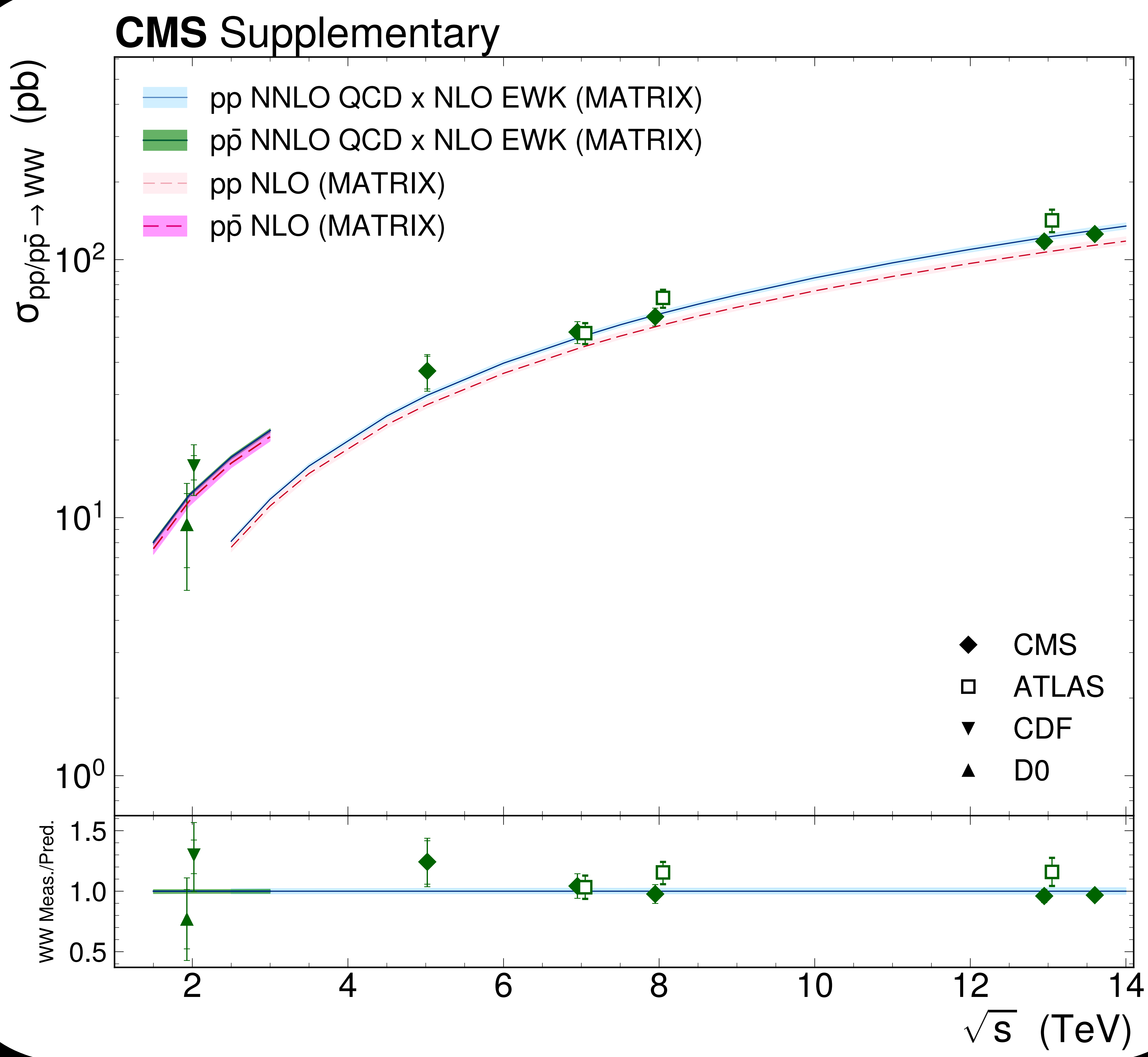

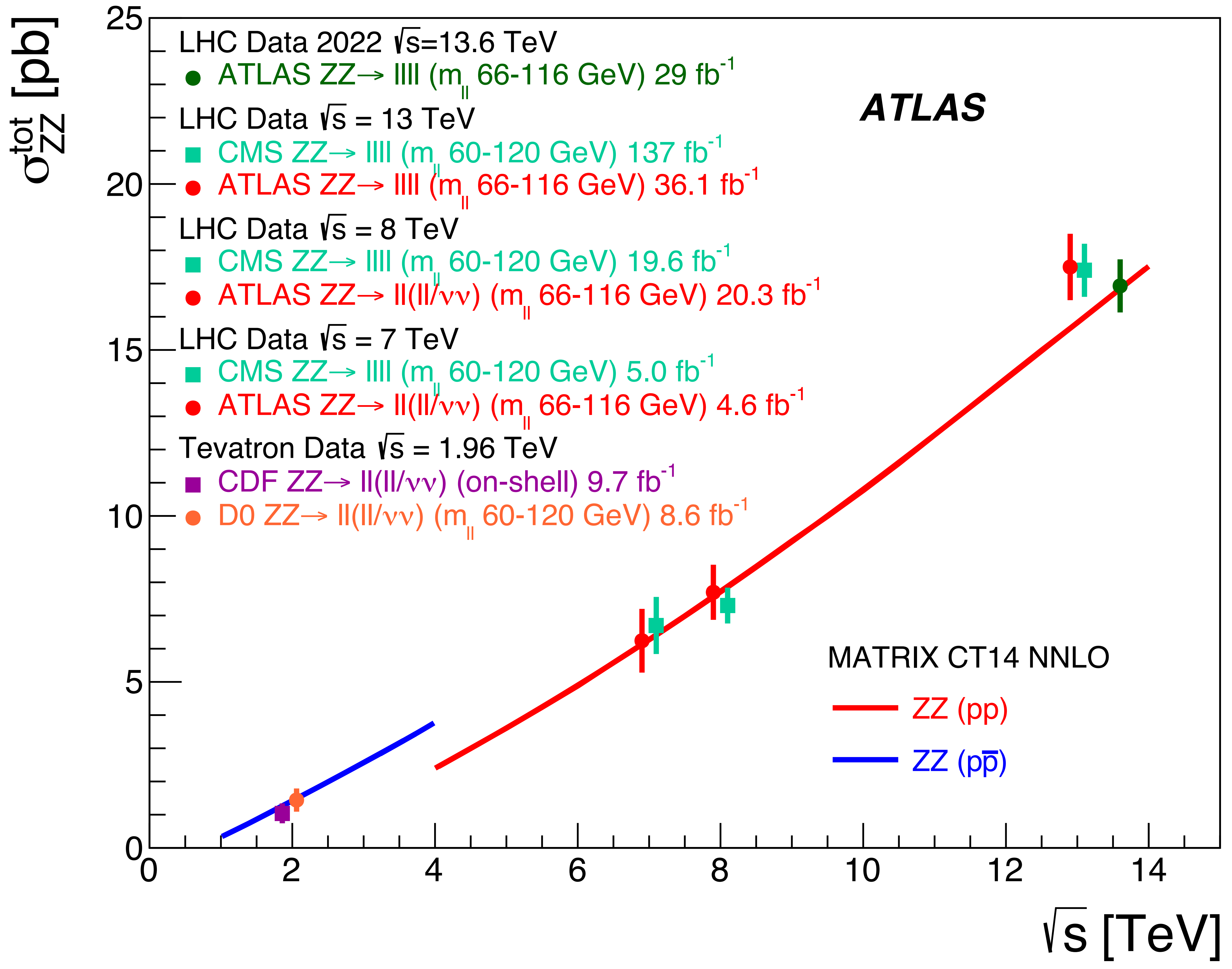

Both ATLAS and CMS have a comprehensive multiboson program, spanning several processes, across orders of magnitude in cross section, allowing us to probe exotic couplings in the Standard Model

Additional Material

VBS WZ at 13 TeV

used to model $W^{\pm}Zjj$ events. The NNPDF3.0NLO [19] parton distribution function (PDF) set was used for the hard-scattering process, while the NNPDF2.3LO [19] PDF set was used for the PS. The dipole recoil scheme [20] is used for the PS. The default dynamic renormalisation and factorisation scales set by MadGraph5_aMC@NLO [21] were used. A first MC event sample, referred to as $WZjj$–EW, includes processes of order six (zero) in α_{EW} (α_{s}). In this sample, which includes VBS diagrams, two additional jets originating from electroweak vertices from matrix-element partons are included in the final state. Diagrams with a b-quark in either the initial or final state, i.e. b-quarks in the matrix-element calculation, are not considered. This sample provides a LO prediction for the $WZjj$–EW signal process. A second MC event sample, referred to as $WZjj$–QCD, includes processes of order four in α_{EW} in the matrix-element. Matrix elements containing three leptons, one neutrino and up to two jets in the final state were calculated at NLO QCD and merged with the PS from Pythia 8.210 using the FxFx scheme [22]. This $WZjj$–QCD sample includes matrix-element b-quarks. Interferences between the $WZjj$–EW and $WZjj$–QCD processes, labelled $WZjj$–INT, include only contributions to the squared matrix-element of order one in α_{s}. Their contribution is simulated at LO in a third MC sample using MadGraph5_aMC@NLO 2.6.5 [16] and the same parameters as used for $WZjj$–EW events. The contribution of interferences is found to be positive and approximately 6% of the $WZjj$–EW cross-section in the fiducial phase space at particle level and maximaly 12% of the $WZjj$–EW cross-section for events with three or more jets of $p_{\mathrm{T}} > 25$ GeV.

VBS WZ at 13 TeV

Dividing the SR in events with $N_{\text{jets}} = 2$ and $N_{\text{jets}} \geq 3$ the $\sigma_{WZjj\text{–EW}}$ and $\sigma_{WZjj\text{–strong}}$ production cross-sections of these two categories of events are measured. The measurements are compared in Figure 5 to the prediction from MadGraph+Pythia8 and Sherpa 2.2.12. For $N_{\text{jets}} \geq 3$, the predicted $\sigma_{WZjj\text{–EW}}$ cross-sections are in good agreement with the measured value while the predicted $\sigma_{WZjj\text{–strong}}$ cross-section lie within about 2σ of the measurement. However, for $N_{\text{jets}} = 2$ the measured $\sigma_{WZjj\text{–strong}}$ cross-section is

lower by a factor of two than the value predicted by both MadGraph+Pythia8 and Sherpa. The predicted values of $\sigma_{WZjj\text{–EW}}$ are found to be in agreement within 1σ of the measured value. The ratio $\mathring{2}3$ of the number of events with $N_{\text{jets}} = 2$ to the number of events with $N_{\text{jets}} \geq 3$ is also extracted from data by the simultaneous fit of the two categories to be $R^{\text{EW}}_{2/3} = 1.70 \pm 0.71$ and $R^{\text{QCD}}_{2/3} = 0.21 \pm 0.06$ for $WZjj$–EW and $WZjj$–QCD events, respectively. In comparison, the values predicted by MadGraph+Pythia8 (Sherpa) are $R^{\text{EW}}_{2/3} = 1.43^{+0.06}_{-0.02}$ (1.67 ± 0.13) and $R^{\text{QCD}}_{2/3} = 0.36^{+0.02}_{-0.04}$ (0.38 ± 0.03), respectively.

The $\sigma_{WZjj\text{–EW}}$ and $\sigma_{WZjj\text{–strong}}$ production cross-sections are measured differentially in three bins of m_{jj}. The measurements are compared in Figure 6 to the prediction from MadGraph+Pythia8 and Sherpa 2.2.12. For $500 < m_{jj} < 1300$ GeV, the MC predictions are found to overestimate the measured

Radiation Amplitude Zero effect in WZ at 13 TeV

At leading-order (LO) in quantum chromodynamics (QCD), WZ production occurs through quark-antiquark interactions in the s-, t-, and u-channels. The dominant helicity amplitude with two transversely-polarized bosons exhibits an exact zero when the scattering angle of the W boson in the WZ rest frame with respect to the incoming antiquark direction approaches 90° [3, 4]. This is a direct consequence of the gauge structure in the SM. This RAZ effect leads to a dip around 0 in the $\Delta Y(WZ)$ and $\Delta Y(\ell_W Z)$ distributions, with $\Delta Y(WZ)$ defined as the rapidity difference between the W and Z bosons, and $\Delta Y(\ell_W Z)$ defined as the rapidity difference between the lepton from the W decay and the Z boson. The RAZ effect has been observed for $W\gamma$ [5–7] for which it is found that the sensitivity for $W\gamma$ resonances is enhanced in this radiation valley [8]. However, the RAZ effect has not yet been observed for WZ due to the W boson polarizations in WZ production [9]. In addition, the next-to-leading order (NLO) QCD corrections dilute the RAZ effect and make it hard to observe experimentally [10, 11]. To reduce jet activity and to increase the significance of the dips, a selection criterion on the transverse momentum of the WZ system (p_T^{WZ}) is applied.

The diboson polarization fractions f_{00}, f_{TT}, f_{0T} and f_{T0} as defined in Ref. [12] are interpreted as probabilities of correlated polarization states of the W and Z bosons. Here, 00 (TT) indicates that both bosons are longitudinally (transversely) polarized, and 0T (T0) indicates that the W (Z) boson is longitudinally polarized and the Z (W) boson is transversely polarized. The ATLAS Collaboration has measured both single and diboson polarization fractions using inclusive WZ events [12], which are dominated by TT events with low momentum W and Z bosons [1, 2, 13]. This analysis focuses on WZ events with Z bosons required to have high transverse momenta (p_T^Z). The combination of high p_T^Z and low p_T^{WZ} significantly reduces the TT contribution and increases f_{00}. As a result, f_{00} increases from $5-7\%$ in the inclusive region to $20-30\%$ in the region with high p_T^Z and low p_T^{WZ} [14].

Random Additional Material

Definition of m_T^{WZ}

$$m_{\mathrm{T}}^{WZ} = \sqrt{\left(\sum_{\ell=1}^{3} p_{\mathrm{T}}^{\ell} + E_{\mathrm{T}}^{\mathrm{miss}}\right)^2 - \left[\left(\sum_{\ell=1}^{3} p_x^{\ell} + E_x^{\mathrm{miss}}\right)^2 + \left(\sum_{\ell=1}^{3} p_y^{\ell} + E_y^{\mathrm{miss}}\right)^2\right]}.$$

https://atlas.web.cern.ch/Atlas/GROUPS/PHYSICS/PAPERS/STDM-2018-31

VBS $W\gamma$ at 13 TeV

- Study of vector boson scattering processes → essential to probe nature of electroweak symmetry breaking
- Electroweak production of $W\gamma jj$: α_{EW}^4
- Differential measurements performed and constraints on various effective field theory operators evaluated
- Observables sensitive to the effect of new physics
  - invariant mass of dijet system (M_{jj}), transverse momenta of two jets (p_T^{jj}), transverse momentum of lepton (p_T^{ℓ}) and invariant mass of the lepton and photon ($m_{\ell\gamma}$)

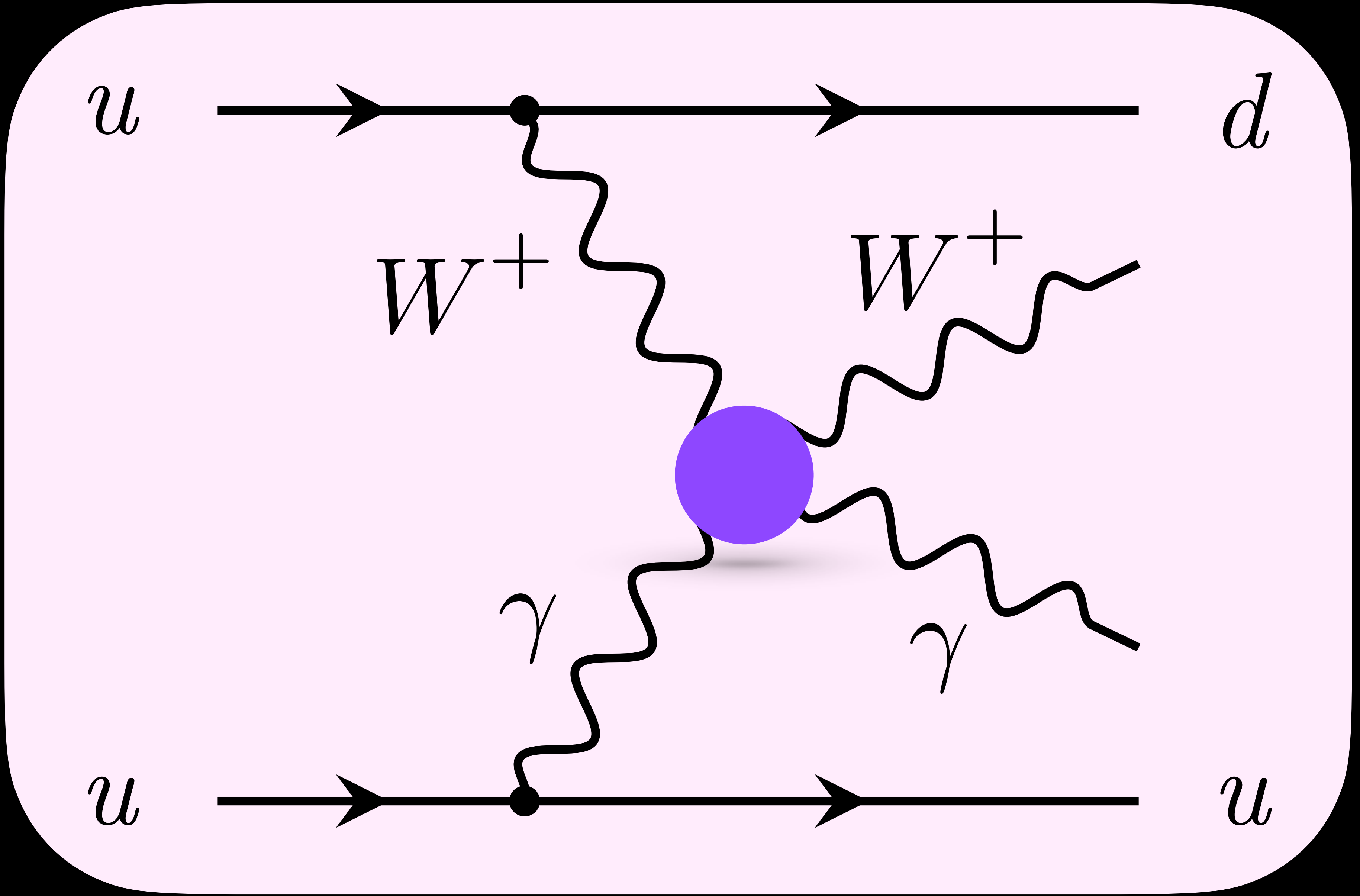

- CP structure of couplings probed with variables $\Delta\phi_{jj}$ and $\Delta\phi_{\ell\gamma}$, where both pairs of objects are ordered by rapidity

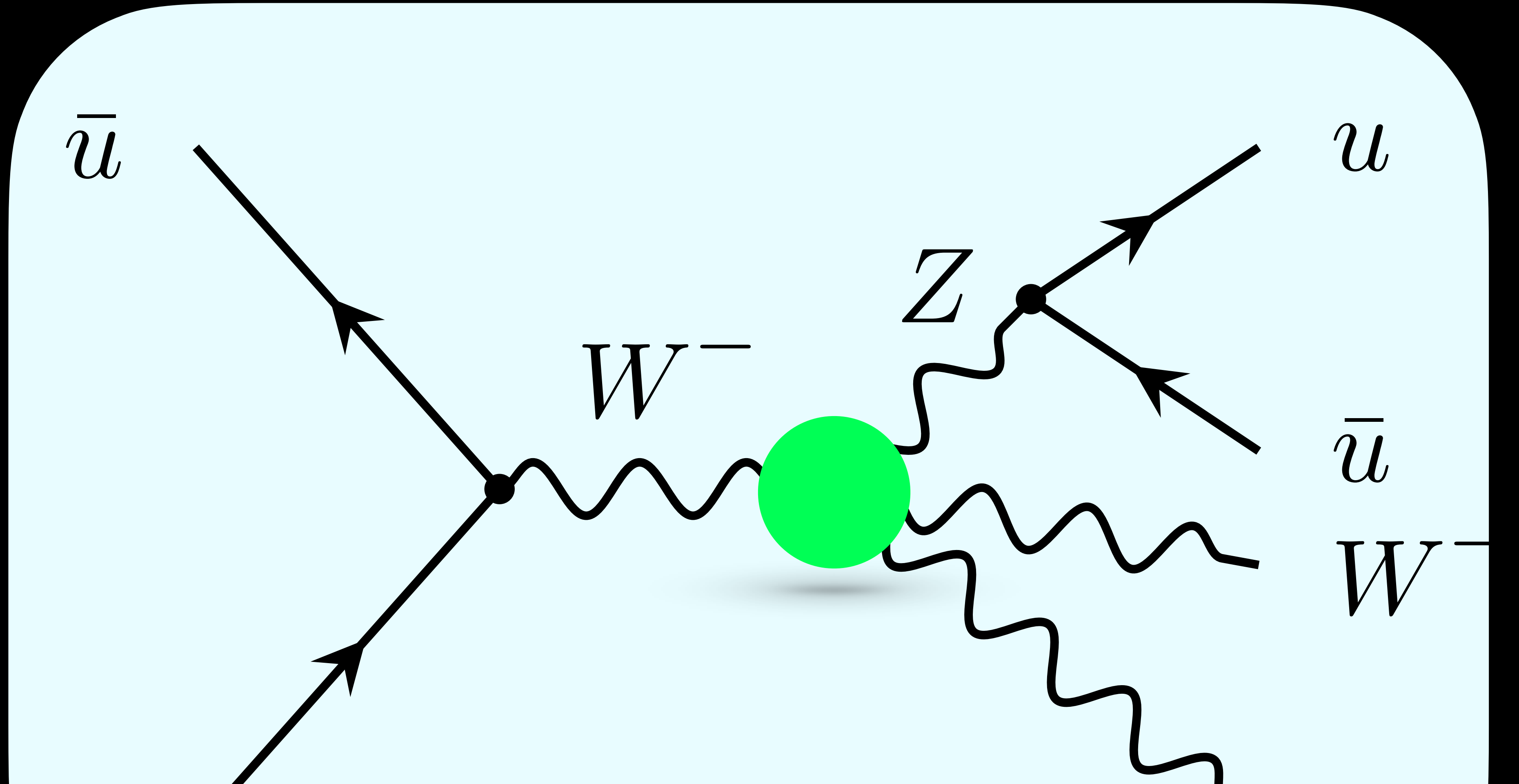

Bremsstrahlung EW $W\gamma jj$ non-VBS production

Previous result: Phys. Rev. D 108 (2023) 032017

Vector Boson Scattering

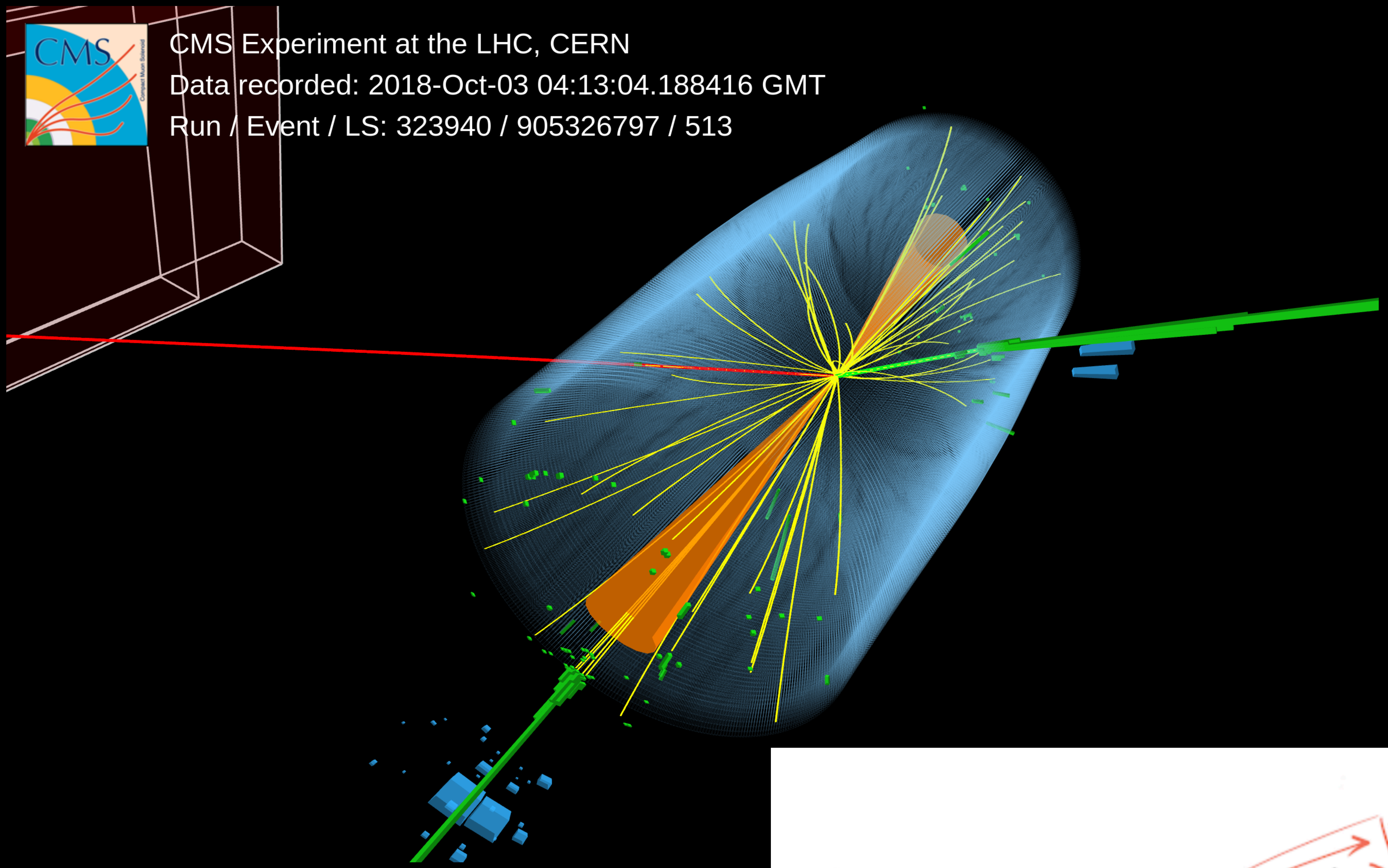

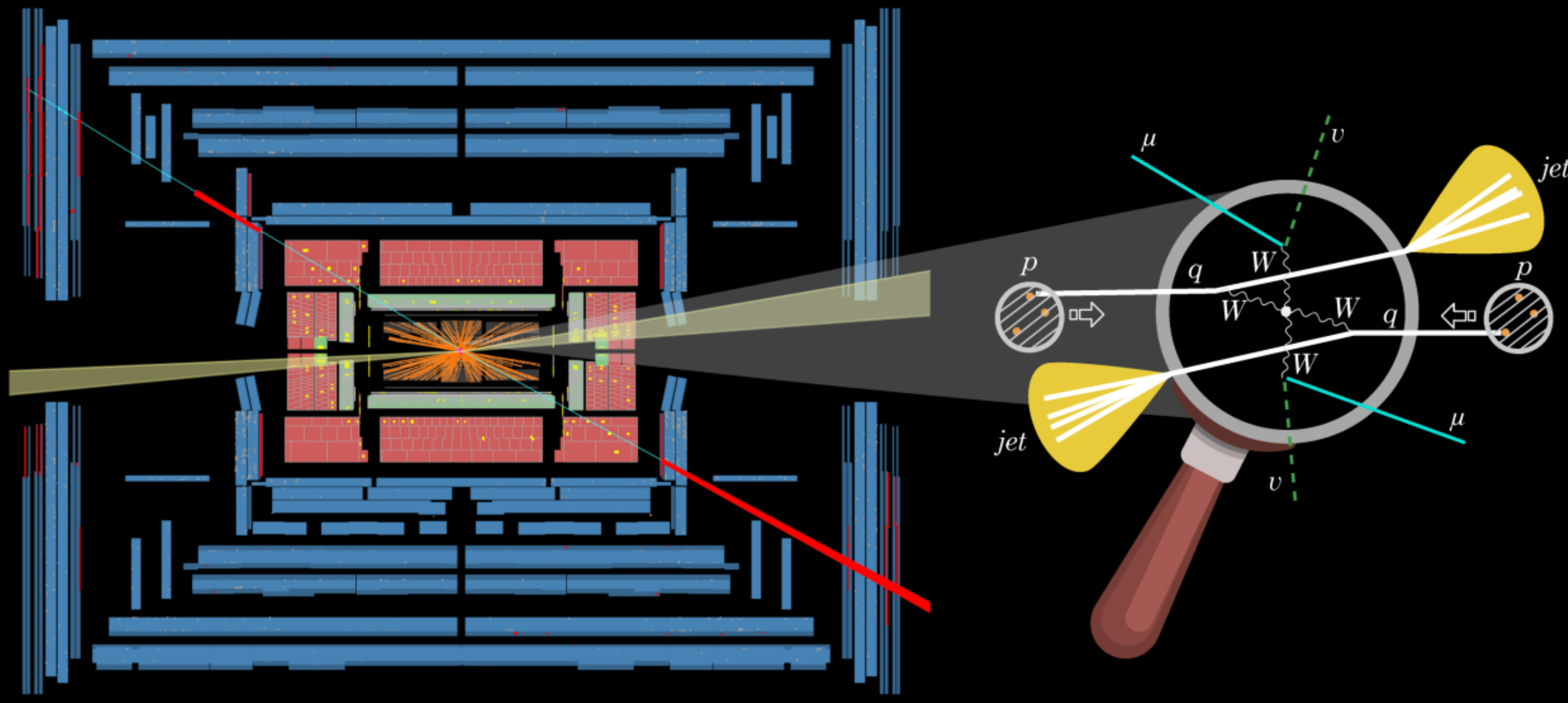

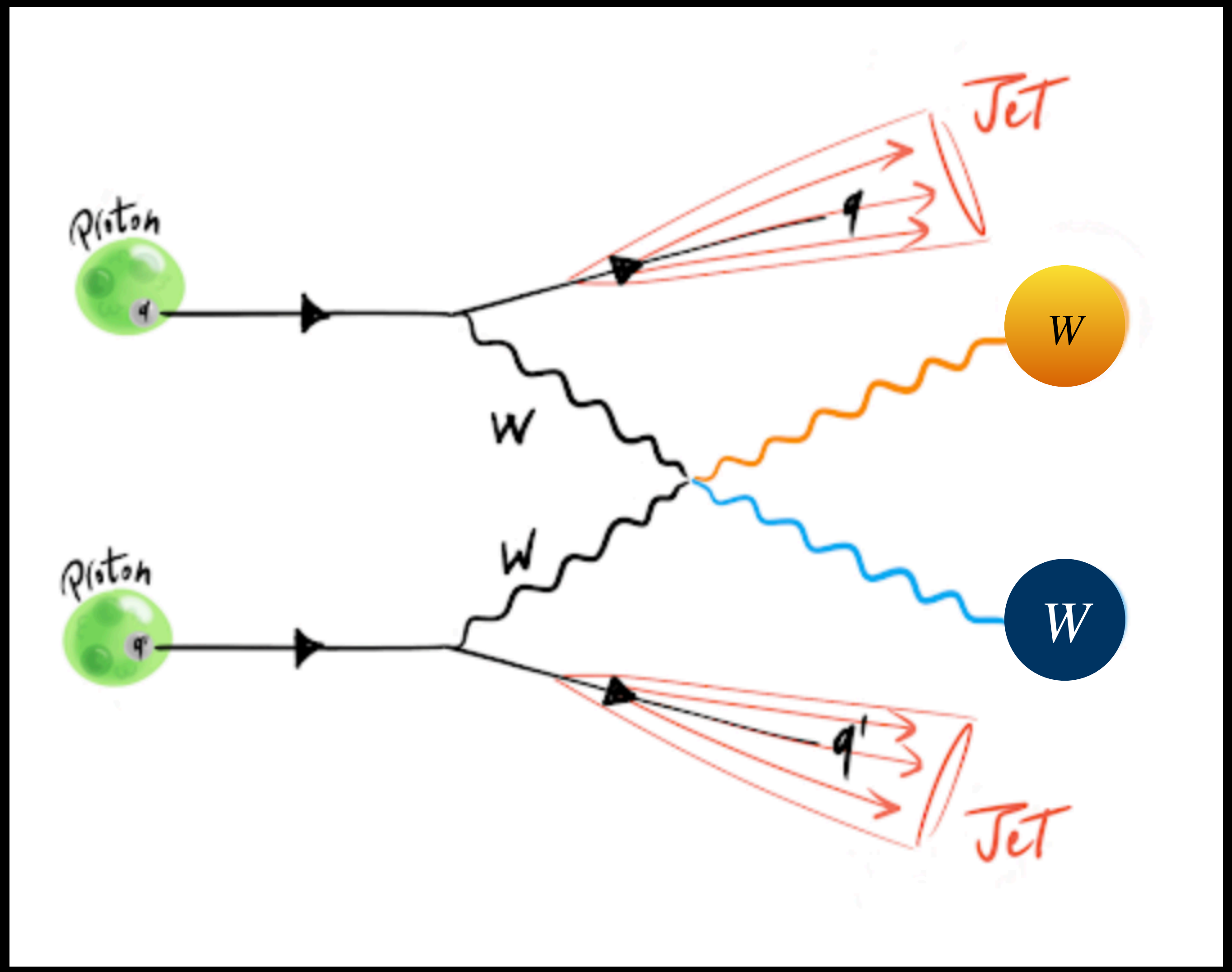

- Pure electro-weak interactions of order (α_{EW}^4)

- Final state consists of two high transverse momenta (p_T) jets
- Rapidity gap between jets → no color flow
- High mass of the two jets (M_{jj})
- Decay product of the gauge bosons: central with respect to jets

Vector Boson Scattering

- Study of vector boson scattering processes → essential to probe nature of electroweak symmetry breaking
- Pure electro-weak interactions of order α_{EW}^4
- Differential measurements performed and constraints on various effective field theory operators evaluated
- Observables sensitive to the effect of new physics
  - invariant mass of dijet system (M_{jj}), transverse momenta of two jets (p_T^{jj}), transverse momentum of lepton (p_T^{ℓ}) and invariant mass of the lepton and photon ($m_{\ell\gamma}$)

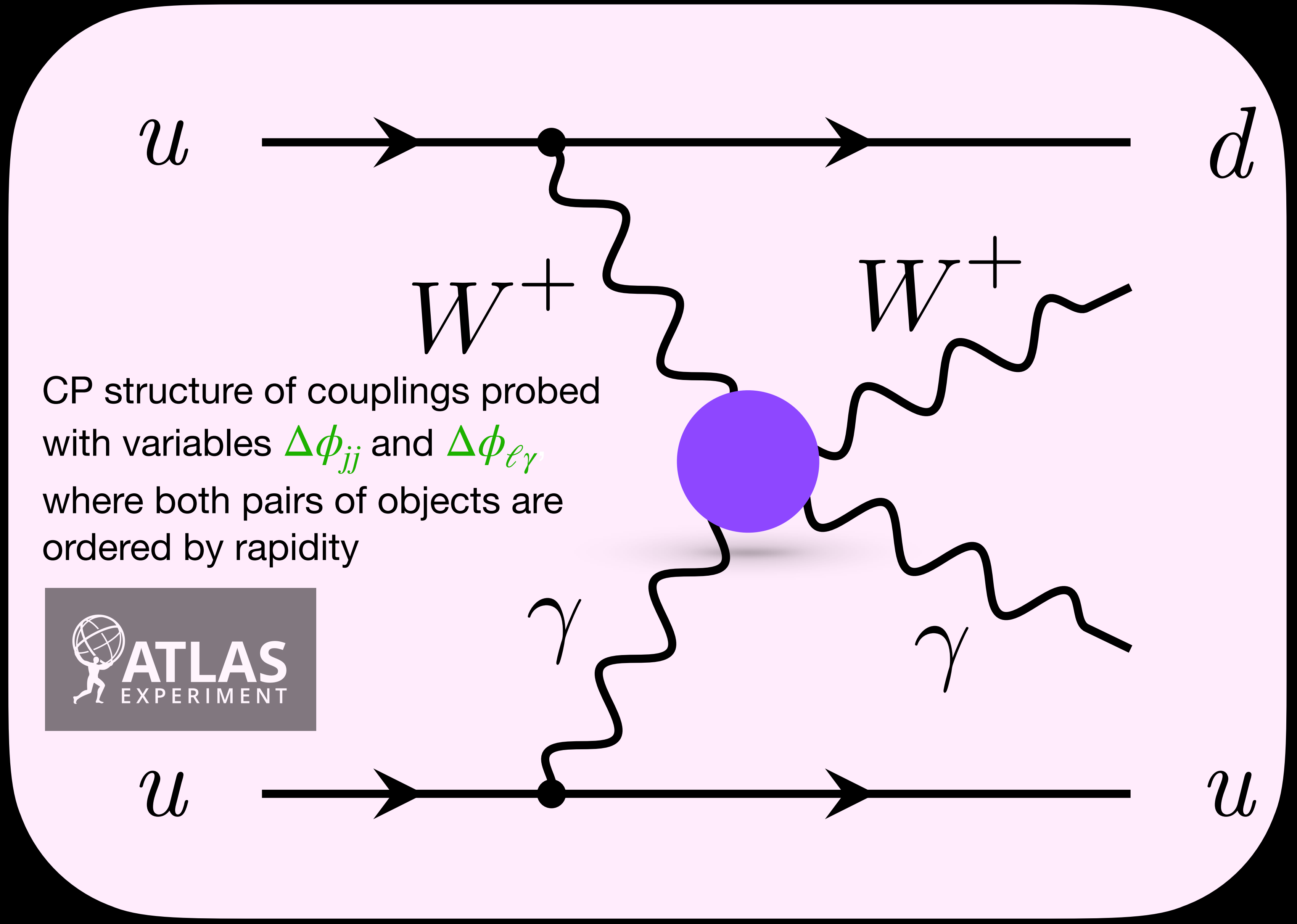

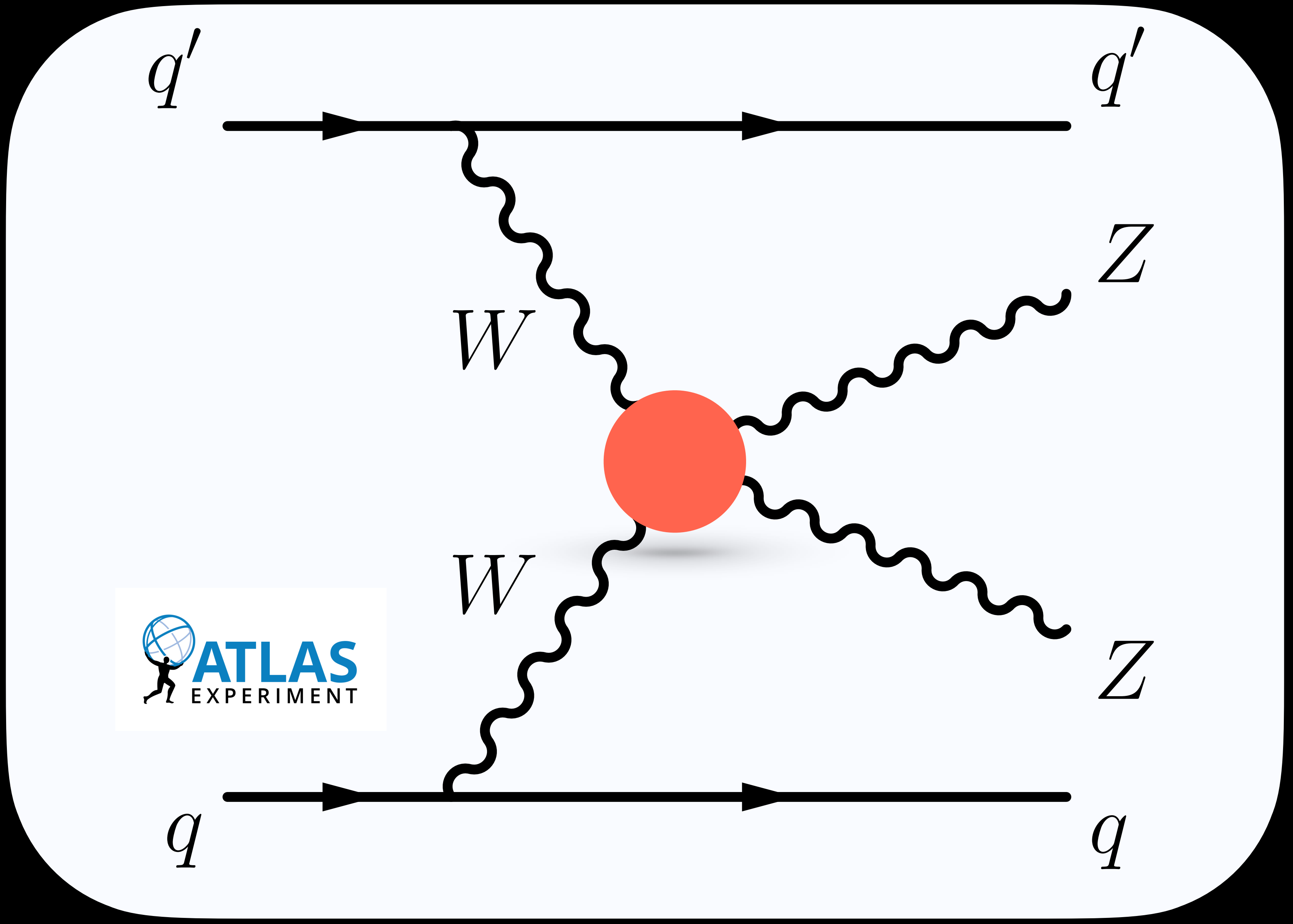

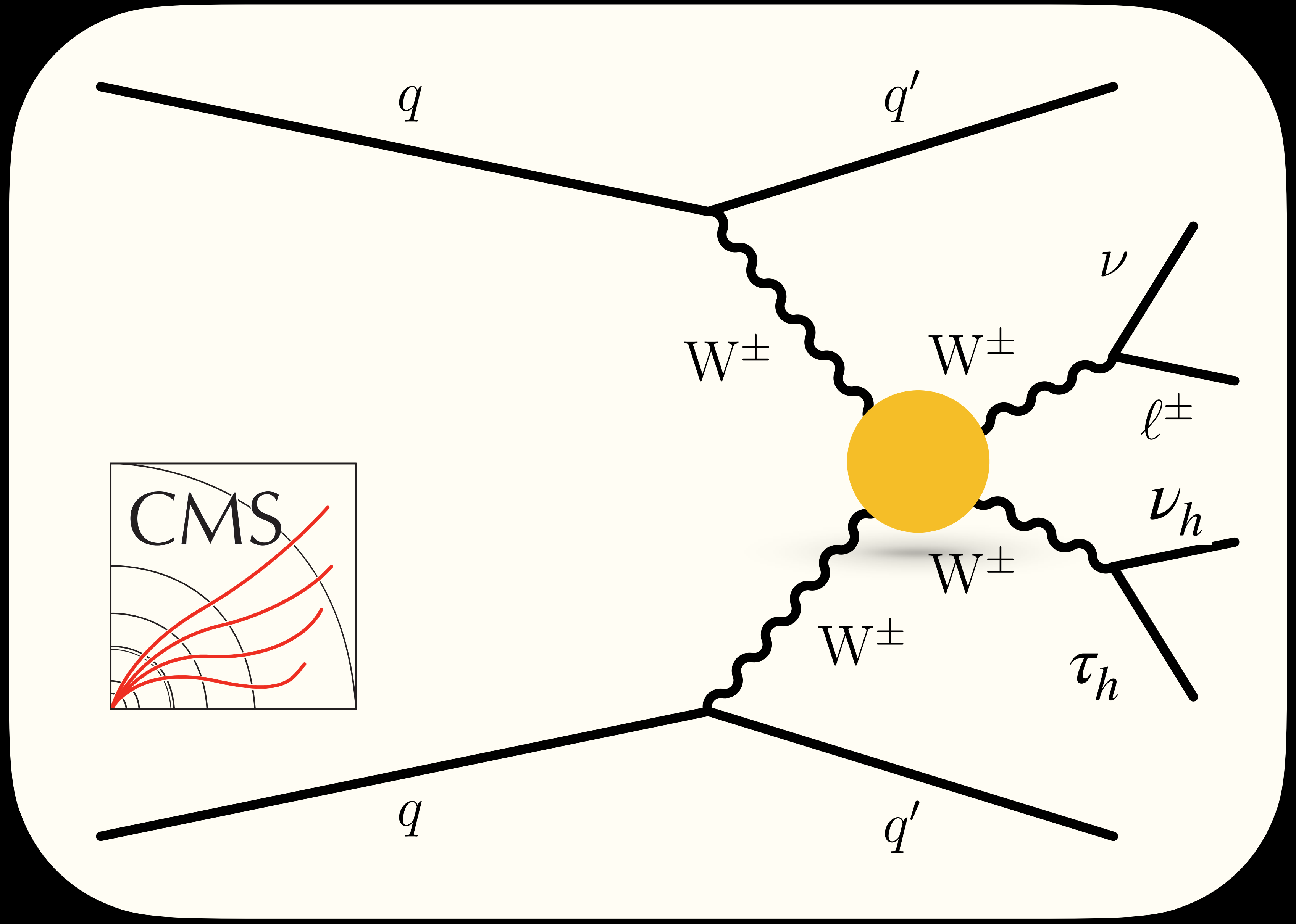

http://cds.cern.ch/record/2867989?ln=en

VBS Same Sign WW with hadronic τ

- Final state where one of the two same-signed W-bosons decays to a hadronic τ
  - Signature: $\tau_h \nu_\tau \ell \nu_\ell (\ell = e, \mu)$
- Evidence of SM process at 2.7 σ, signal strength: $1.44^{+0.63}_{-0.56}$
  - Public since August 2023

Signal Region → Same sign ℓ, τ_h pair → $p_T^{miss} > 50$ GeV, $m_{jj} > 500$ GeV, Veto on b-tagged jets

Several Control Regions → Opposite sign pair | Top control region | Fakes

VBS Same Sign WW with hadronic τ

$$N \propto |\mathcal{A}|^2 = |\mathcal{A}_{SM}|^2 + \sum_{\alpha} \frac{C_\alpha}{\Lambda^2} . \mathcal{R}e(\mathcal{A}_{SM} \mathcal{A}^{(6)\dagger}_{Q\alpha}) + \sum_{\alpha,\beta} \frac{C_\alpha C_\beta}{\Lambda^4} . (\mathcal{A}^{(6)}_{Q\alpha} \mathcal{A}^{(6)\dagger}_{Q\beta}) + \sum_k \left[\frac{f_k}{\Lambda^4} . 2\mathcal{R}e(\mathcal{A}_{SM} \mathcal{A}^{(8)\dagger}_{Q_k}) \right]$$

Dim6 including linear, BSM and mixed contributions

Dim8 including linear contributions

$$+ \sum_k \frac{f_k^2}{\Lambda^8} . (\mathcal{A}^{(8)}_{Qk} \mathcal{A}^{(8)\dagger}_{Qk})$$

Dim8 BSM contribution

- Several dim-6 (11) and dim-8 (9) operators explored
- Transverse mass (M_{01}) used as the variable of interest
  - Most sensitive variable

$$M_{01} = (p_{T\tau} + p_l + \vec{p}_T^{\,miss})^2 + |p_{T\tau} + \vec{p}_T^{\,miss}|^2$$

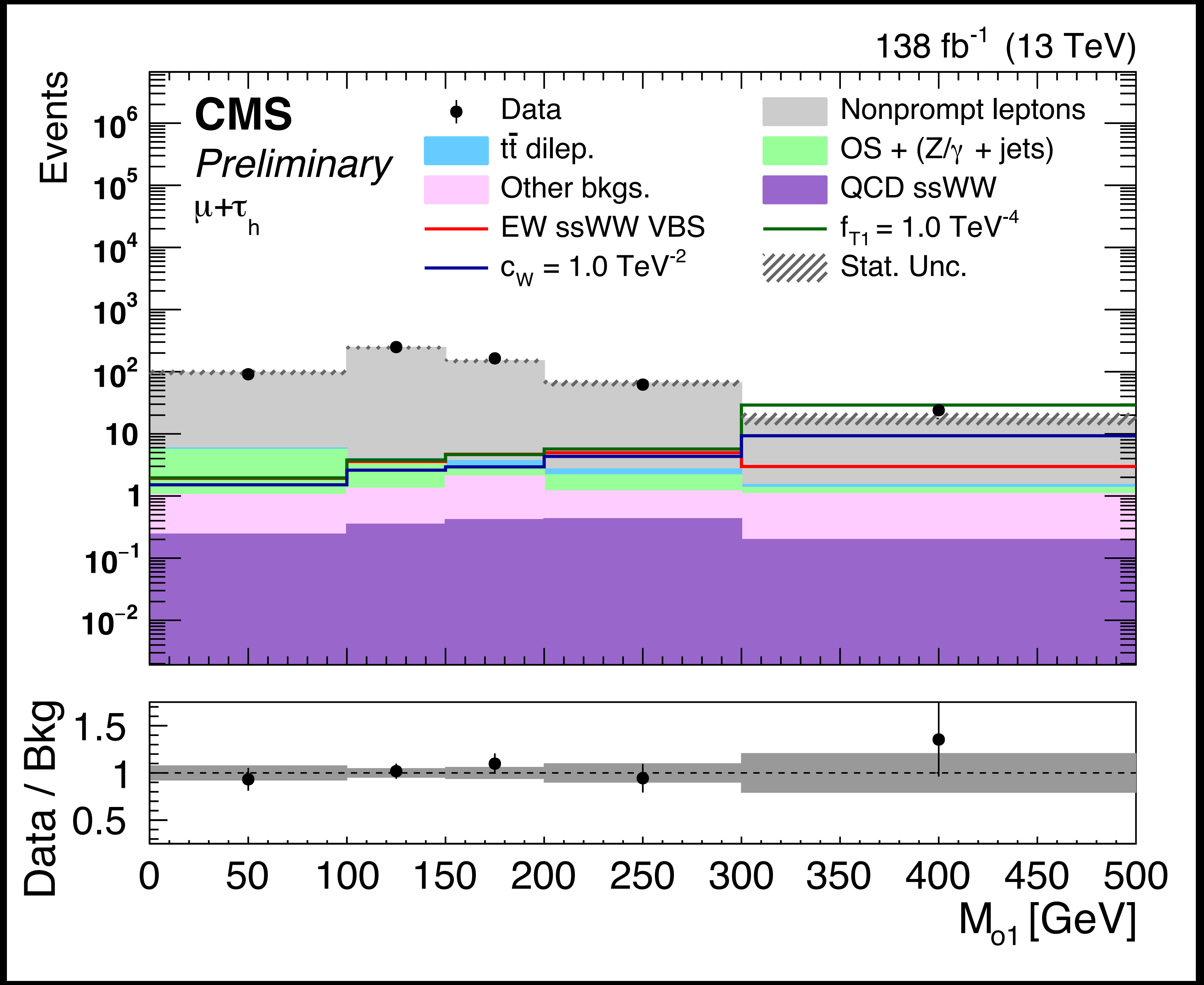

W^+W^- cross section measurement at 13.6 TeV

- First measurement of W^+W^- at 13.6 TeV
- Used data collected in 2022 → 34.8 fb^{-1}
- Event category: 1 muon and 1 electron of opposite charge
- The inclusive cross section is 125.7 ± 5.6 pb, in agreement with predictions

Additional $WZ \to 3\ell\nu$ and $ZZ \to 4\ell$ control regions (CRs) defined

Quantity
Number of t
Additional l
Lepton char
$p_T^{\ell\,\max}$
$p_T^{\ell\,\min}$
$m_{\ell\ell}$
$p_T^{\ell\ell}$
Number of b
N_J

	Same-sign CR	$Z \to \tau\tau$ CR	One b-tag CR	Two b-tag CR
Data	3456	56551	68656	57617
WW	81.7 ± 9.5	2662 ± 94	2220 ± 180	248 ± 54
Top quark	87.3 ± 8.4	1126 ± 34	63340 ± 750	55610 ± 620
$Z \to \tau\tau$	57.0 ± 9.3	45630 ± 590	227 ± 27	19.6 ± 7.9
WZ	512 ± 24	97.6 ± 4.9	96.9 ± 6.3	11.8 ± 1.7
ZZ	33.6 ± 1.7	66.0 ± 3.9	6.9 ± 0.5	1.0 ± 0.1
Nonprompt	2390 ± 130	6550 ± 440	2630 ± 270	1640 ± 220
VVV	25.8 ± 1.3	4.7 ± 0.4	33.7 ± 2.1	8.7 ± 0.8
tVx	8.7 ± 2.7	0.7 ± 0.1	44.1 ± 3.2	52.1 ± 3.3
$V\gamma$	232 ± 19	69.2 ± 7.6	43.2 ± 9.5	3.1 ± 0.9
Higgs	27.5 ± 5.2	344 ± 52	29.3 ± 4.8	20.7 ± 3.2
Total	3460 ± 130	56550 ± 420	68670 ± 560	57610 ± 490

https://arxiv.org/abs/2403.02809

VBS $W\gamma$ at 13 TeV

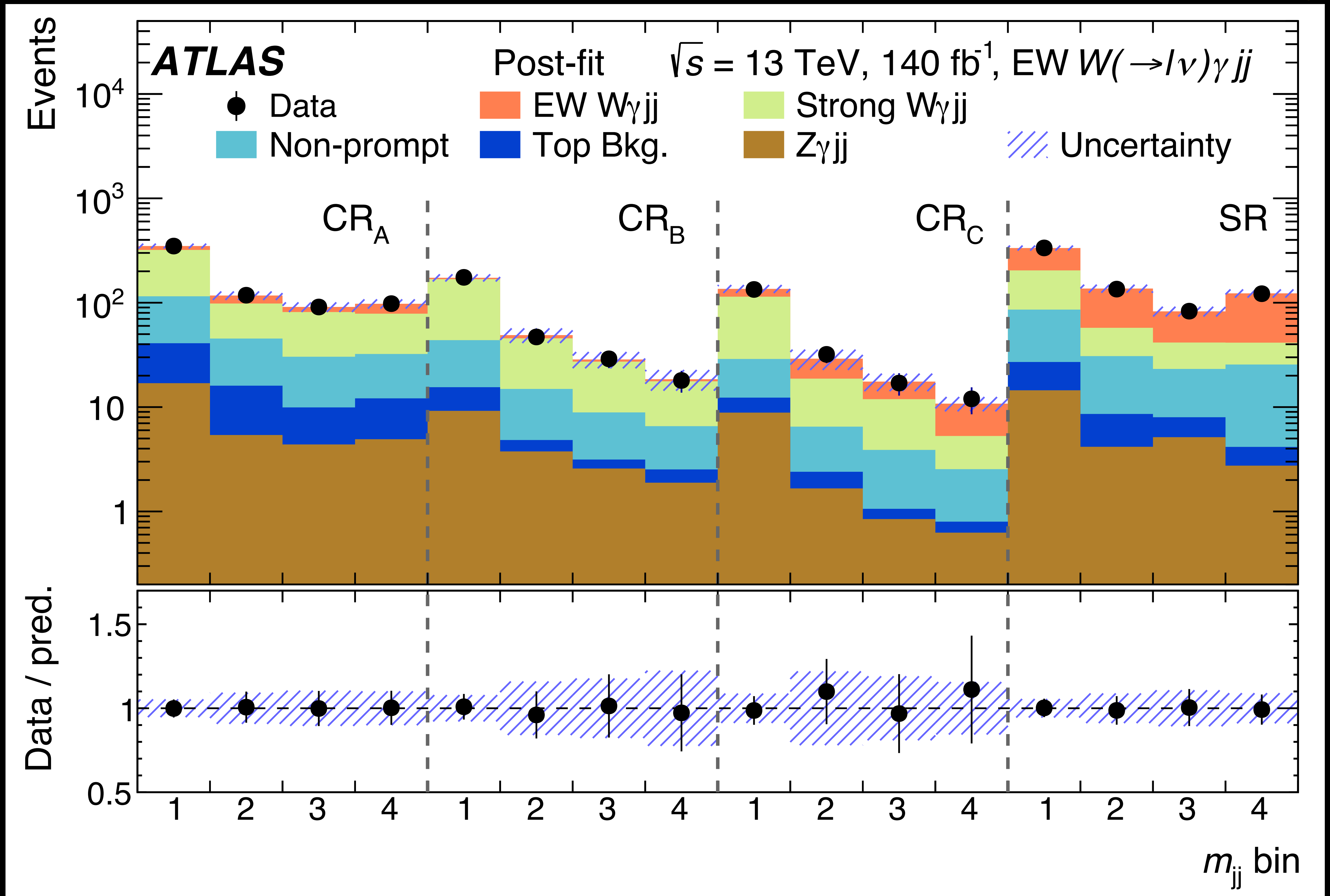

CRA: $N^{\text{gap}}_{\text{jets}} > 0$, $\xi_{\ell\gamma} < 0.35$

CRB: $N^{\text{gap}}_{\text{jets}} > 0$, $0.35 < \xi_{\ell\gamma} < 1$

CRC: $N^{\text{gap}}_{\text{jets}} = 0$, $0.35 < \xi_{\ell\gamma} < 1$

The ABCD method is only used in the differential measurement

	$\text{SR}^{\text{fid}}\left(N^{\text{gap}}_{\text{jets}} = 0\right)$	$\text{CR}^{\text{fid}}\left(N^{\text{gap}}_{\text{jets}} > 0\right)$
EW $W\gamma jj$	520 ± 141	120 ± 49
Strong $W\gamma jj$	1550 ± 830	1970 ± 950
Non-prompt	692 ± 57	698 ± 58
Top quark processes	109 ± 18	183 ± 37
EW + strong $Z\gamma jj$	128 ± 34	163 ± 77
Total	3000 ± 830	3140 ± 960
Data	3341	3143

Highest ranked variables

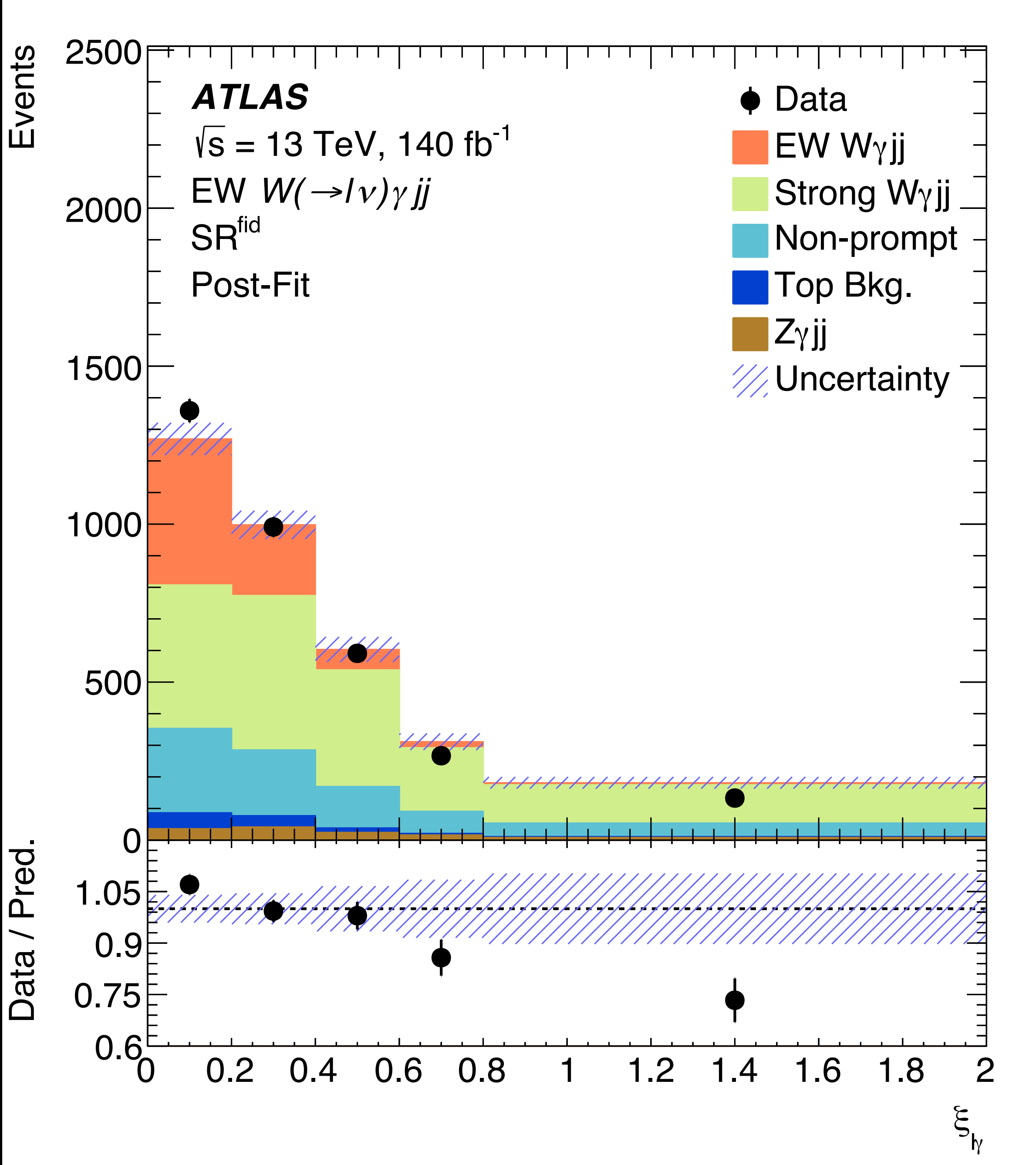

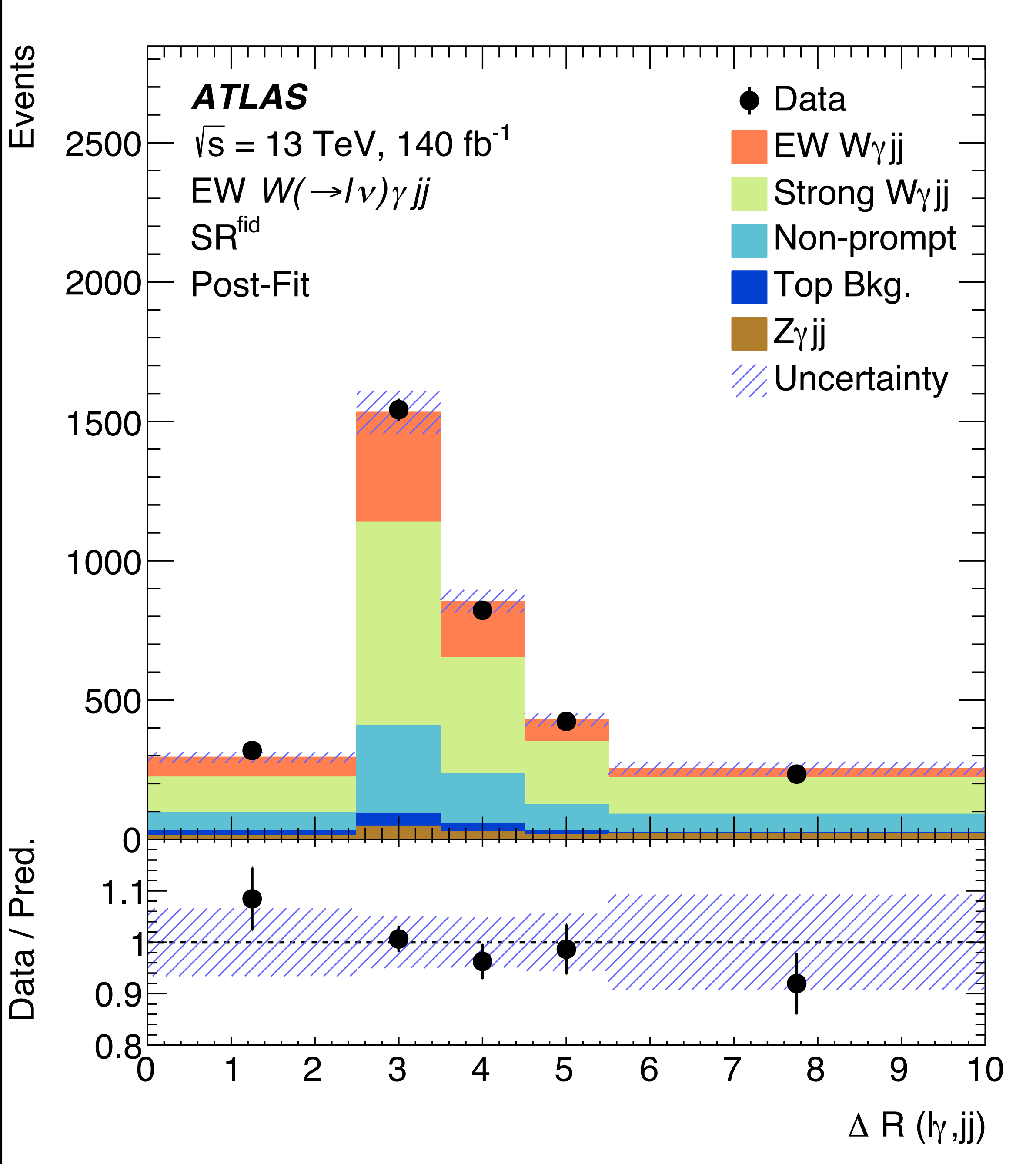

- Signal region (SR) and control region (CR) defined by counting $N^{\text{gap}}_{\text{jets}}$ (rapidity interval between the two leading jets)
  - SR: $m_{jj} > 1$ TeV, $\xi_{\ell\gamma} = \left| \left(y_{\ell\gamma} - \frac{(y_{j_1} + y_{j_2})}{2}\right) / (y_{j_1} - y_{j_2}) \right| < 0.35$
- Neural Network trained with 13 angular and kinematic variables used to enhance sensitivity to EW $W\gamma jj$ (inclusive measurement)